

THESIS

THE KINETICS OF PROTEINS ON LIPID BILAYERS

Submitted by

Kanti Nepal

School of Biomedical Engineering

In partial fulfillment of the requirements

For the Degree of Master of Science

Colorado State University

Fort Collins, Colorado

Summer 2017

Master's Committee:

Advisor: Diego Krapf

Olve Peersen

Nancy Levinger

Copyright by Kanti Nepal, 2017
All Rights Reserved

ABSTRACT

Signaling molecules trigger downstream signaling pathways when they arrive at the plasma membrane. They have to be recruited to the plasma membrane by membrane targeting domains. Our experiments throughout focus on understanding kinetics of C2 domain's diffusion on the membrane. In contrast to trans-membrane proteins, interactions between these domains and the plasma membrane is found to be peripheral and transient. These proteins perform two dimensional diffusion on membrane surfaces and faster three dimensional diffusion in the bulk. We label proteins at the single molecule level and do single particle tracking. In addition to two dimensional surface diffusion, it is sometimes observed that they dissociate from the membrane and rebind at a another location of the membrane after a short journey in the bulk solution. The time averaged mean square displacement (MSD) analysis of individual trajectories is linear whereas ensemble average MSD is superdiffusive. The distribution of displacements fit to a Gaussian distribution followed by a long tail which is Cauchy's distribution. This long tail in cauchy's distribution is from the larger displacements caused by jumps of molecule to explore greater area for efficient target search. The second section of this thesis explored the effect of crowding agents on these proteins. Polyethylene glycol (PEG) is used here to simulate crowded cellular environment aiming to understand its effect on membrane targeting C2 domains as well as on the lipid bilayer. In this chapter, we recognized that a crowding agent like PEG plays a significant role in changing the trend on diffusion behavior of C2 domains. When the PEG concentration is increased, there is a decrease in the transition of molecule between the surface and the bulk phase. With the same series of PEG concentration, there is increase in population of immobile C2 domains and desorption time. But no such increasing or decreasing trend is seen on the lipid bilayer alone. Experiments were reproduced and imaged a number of times using total internal reflection (TIRF) and fluorescence recovery after photobleaching (FRAP) techniques. Lastly, a small part of my thesis also dealt with set of experiments done to monitor tethered particle motion of DNA as well as flow extension experiments on DNA and RNA using bright field microscopy. DNA/RNA had beads tethered to one end of the strand and other end to the cover glass. Primary results are presented.

ACKNOWLEDGEMENTS

I would like to express my sincere gratitude to my advisor *Dr. Diego Krapf* for his constant support on my thesis. I thank him for his kind and motivating supervision. His guidance and immense knowledge helped me during the period of research and writing this thesis.

I would like to thank *Dr. Olve Peersen* and *Dr. Nancy Levinger*, for being part of the committee and providing their insightful comments and support.

I would like to express sincere thanks to Grace Campagnola, Bryce Schroder, Sanaz Sadegh and Xinran Xu for all their guidance and support during my research at CSU. I would also like to express my sincere gratitude to my parents, sister, my brother in law and my beloved boyfriend for encouraging and supporting me towards my higher studies. I would like to thank all of my Nepalese friends at CSU, who supported me. I thank you all for your time and wonderful company.

TABLE OF CONTENTS

ABSTRACT	ii
ACKNOWLEDGEMENTS	iii
LIST OF FIGURES	vii
Chapter 1 INTRODUCTION	1
1.1 Objective and motivation	1
1.2 Outline	2
1.3 Fatty acids, phospholipids and membrane composition	3
1.4 Design and model system of in vitro built bilayers	3
1.5 Macromolecular crowding	4
1.6 Fluorescence, microscopy and instruments	5
1.6.1 Total internal reflection fluorescence microscopy (TIRF)	5
1.6.2 Florescence recovery after photo bleaching(FRAP)	5
1.6.3 Acoustic force spectroscopy (AFS)	7
1.7 Nucleic acid biology	8
1.7.1 DNA structure and function	8
1.7.2 RNA structure and function	9
Chapter 2 MOTION OF MEMBRANE TARGETING C2 DOMAINS ON SYNTHETIC LIPID BILAYER	10
2.1 Introduction	10
2.2 Methods and materials	12
2.2.1 Sample preparation	12
2.2.2 Instrumentation and software	14
2.3 Results	15
2.4 Discussion and conclusion	19

Chapter 3	INFLUENCE OF CROWDING AGENT ON LIPID BILAYERS IN PRESENCE AND ABSENCE OF PROTEINS	21
3.1	Introduction	21
3.2	Methods and materials	23
3.2.1	Sample preparation	23
3.2.2	Instrumentation and software	23
3.3	Results and discussion	25
3.3.1	Effect of PEG on C2 domains	25
3.3.2	Effect of PEG on lipids	30
3.4	Conclusion	35
Chapter 4	TETHERED PARTICLE MOTION OF DNA AND RNA WITH RNA EXTENSION EXPERIMENT	38
4.1	Introduction	38
4.1.1	Purpose of experiment	38
4.2	Methods and materials	40
4.2.1	Surface passivation	40
4.2.2	Flow based chamber preparation	40
4.2.3	Working of sample transfer setup	40
4.3	Results	41
4.3.1	Tethered particle motion of beads tethered to DNA and DNA stretching	41
4.3.2	RNA extension mechanism and experiment	43
4.3.3	Amplitude measurement of tethered beads	45
4.4	Discussion and conclusion	46
Chapter 5	CONCLUSION AND FUTURE WORKS	47
	Bibliography	49
Appendix A	MATERIALS LIST AND PROTOCOLS	57
A.1	Surface etching for lipid bilayer	57
A.2	Cleaning Chamber wells	58

A.3	Preparing the lipids - one day earlier and day of experiment	59
A.4	Preparing Buffer	61
A.5	Preparing imaging setup	62
A.6	Conducting C2 domains and C2-GST control Experiment	63
A.7	Preparing PEG solution	65
A.8	Conducting experiment on C2 domains with crowding agent	66
A.9	Conducting FRAP experiment	67
A.10	Surface passivation for TPM and RNA extension experiment	69
A.11	APTES (Amine propyl triethyl silane) coating	71
A.12	1 st round of passivation	73
A.13	2 nd round of passivation	75
A.14	Making a flowcell	77
A.15	Conduct Tethered Particle motion (TPM) experiment	79
A.16	AFS chip surface passivation	81
A.17	AFS experiment buffer preparation	84
A.18	Making AFS lookup table	85

LIST OF FIGURES

Figure 1.1	Components of crowded cell environment	5
Figure 1.2	Schematic diagram of TIRF microscopy	6
Figure 1.3	FRAP method	7
Figure 1.4	Acoustic Force Spectroscopy chip	8
Figure 2.1	Diffusion Process	12
Figure 2.2	Experimentation	15
Figure 2.3	Single particle tracking	16
Figure 2.4	Anomalous diffusion analysis of C2 domains (monomer and dimer)	18
Figure 3.1	Distribution of displacements	29
Figure 3.2	Distribution of diffusion coefficients	30
Figure 3.3	Effect of PEG on C2 domains	31
Figure 3.4	Flourescent lipid for FRAP experiment	32
Figure 3.5	Intensity recovery in FRAP w.r.t series of PEG concentration	33
Figure 3.6	Results from FRAP experiment	34
Figure 4.1	DNA stretching and recoiling in response to flow	44
Figure 4.2	RNA stretching in response to increased flow rate	45

INTRODUCTION

1.1 Objective and motivation

The idea of membrane targeting domains is that these domains appear in membrane proteins, so that proteins can bind to the membrane. Many types of signaling molecules have a membrane binding domains because of which it goes and docks at specific membrane. Diffusion behavior of such molecule on solid-liquid or liquid-liquid interfaces are interesting to look at, especially when it plays a vital role in real life applications. For instance making functional bioinspired surface depends significantly on how molecules on these surfaces interact with each other to essentially fulfill its purpose [1]. Another example could be developing a biomaterial based organ implant or where biocompatibility comes into play. We have to look into the interaction of that implant with the inner body environment [2]. This is again looking into solid liquid interface where molecules diffuse around and find the appropriate binding sites. Biosensor development is another motivational field where outcomes from this thesis research could be helpful [3]. Heart valves, catheters, hemodialysis membranes and many more blood contacting devices are some of the good examples [4]. Development of such life saving inventions usually have undergone the diffusion behavior analysis so that its interaction with surface and the bodily fluid can be understood. Keeping this long term goal in mind, the objective of my thesis is set to understand the diffusion behavior of C2 domains. Our experiment is on membrane targeting protein named synaptotagmin7. Synaptotagmin7 has transmembrane N terminal which inserts itself into the synaptic vesicle which has to be recruited [5]. The C terminal of synaptotagmin7 has 2 domains named C2A and C2B. The N - C terminals are connected by the linker. Particularly, our experiments are on Synaptotagmin7 C2A domains. C2 domains are activated in presence of calcium which brings conformational changes in the linker [5]. This phenomenon bring C2 domains at the membrane to trigger the process of vesicle fusion [6]. In case of synaptotagmin7 C2 domains, this happens in two mechanism. First one is when C2 domains binds to calcium which further

binds to anionic membrane with electrostatic interaction. Second is the mechanism in which C2 domains penetrates a bit into the membrane due to hydrophobic interactions. Because of this two step docking mechanism, the retention time of Synaptotagmin7 C2 domains are longer on lipid membranes [6]. Further, these experiments were extended to understand the behavior of C2 proteins in presence of macromolecular crowding on Synthetic Lipid Bilayers. This experiment was done to understand how the C2 domains would behave in crowded cell environment as shown in figure 1.1. Crowded cell environment have components like peripheral proteins, glyco proteins and transmembrane proteins etc.

1.2 Outline

In Chapter 1, I have a brief introduction to the basics related to my research. I also discussed objectives and motivation to choose this topic as my thesis work.

In Chapter 2, I reviewed briefly on introducing the C2 domains and a Control C2- GST. I proceeded to discuss methods and materials used to conduct this research followed by the results obtained. I concluded in this chapter with a discussion on how to interpret the obtained results and conclusion.

In Chapter 3, I gave a brief introduction on crowding agents used. Further we explained how volume exclusion plays a role in anomalous diffusion. I discussed on methods, materials used and continued to results. Discussion and conclusion on the obtained results will follow.

In Chapter 4, I presented a brief introduction on DNA and RNA. Then I discussed the methods and materials used to conduct this experiment. I was able to obtain few understandable results from these experiments leaving a lot of possible future work.

In Chapter 5, I summarized my thesis. Based on the results obtained, I drew overall conclusions and discussed how each experiment has its possible future work. I also mentioned how it can be improved and continued in the future.

1.3 Fatty acids, phospholipids and membrane composition

Similar to the majority of the lipids in membranes, phospholipids have both non-polar and polar regions meaning they are amphiphilic in character. The design of hydrophobic and hydrophilic regions drives the mechanism of formation of lipid bilayer membrane. The polar head groups are formed from many types of organic compounds as glycerol, serine, choline, ethanolamine. Choline and ethanolamine do not have net charge but glycerol and serine have negative charge because of their phosphate group. The non-polar tail groups are hydrophobic compounds due to the fatty acid tail.

The fatty acid tail is composed of a string of carbons and hydrogen. It has a kink in one of the chains when it is a double-bond structure. Fatty acids are long-chain hydrocarbon molecules containing a carboxylic acid moiety at one end, such as RCOOH where R is a long hydrocarbon chain. The numbering of carbons in fatty acids on the number of the carbon in carboxylate group followed by the number of unsaturated sites. Fatty acids that does not have carbon-carbon double bonds are saturated fatty acids and the ones with double bonds are unsaturated fatty acids. The numeric designations used for fatty acids come from the number of carbon atoms. The variety a fatty acids is named to the phospholipids and helps us know the fatty acid composition. For example, a phospholipid containing two palmitic acids (16 carbons each) and a choline group is called dipalmitoyl phosphatidylcholine (DPPC) [7]. The other phospholipids are phosphatidylcholine (PC), phosphatidylethanolamine (PE), phosphatidylserine (PS), phosphatidylglycerol (PG). In this thesis we used PC, PS, PE.

1.4 Design and model system of in vitro built bilayers

Plasma membrane of a normal cell has three layers [8]. The external layer is covered with glycocalix which is a film of branched polypeptide head groups of the glycoproteins and oligosaccharides. The central layer has liquid lipids and proteins. The internal layer has the bilayer joined to cytoskeleton network, usually actin [9]. Building an in vitro setup to try to duplicate in vivo environment is a challenge because we are trying to create a

similar biological content of lipids on our experimental surface. Cellular environment are crowded due to presence of lipids and proteins as shown in figure 1.1. Most of the time experiments have to be done on a glass surface, plastic surface, closed well chamber, flow cell or coated surfaces which might or might not be good enough to replicate a of real membrane. Building an in vitro setup is building a model system which allows us to understand a particular phenomenon in an environment where it is isolated from other proteins [10]. Model membranes for these experiments are just good enough for simulation of cellular plasma membrane without other proteins. In vivo cellular plasma membranes are too complex where direct revelation of particular mechanisms becomes challenging. Model membrane gives us a precise control of the setup we need. There are a variety of methodologies to design and make it. Supported lipid bilayers is our model system where we make use of a solid support underneath the lipid bilayer. Our support here is the cleaned/etched glass surface. Mixing of samples, cleaning the bilayer, adding of crowding agents as well as imaging of samples is easier with solid support because it provides a flat local plane and resistance to the force induced by multiple pipetting. [11] . Broadly speaking, the results from our model system, the supported lipid bilayer are understood and interpreted in such a way that the comparison can be made with in actual cellular system.

1.5 Macromolecular crowding

The internal environment of a cell is a crowded. To mimic the in vivo environment we added crowding agent (PEG) in vitro to understand kinetics of proteins. Diffusion of proteins on lipid bilayer as well as the hopping events are affected by crowding agents [12]. This is caused by macromolecular crowding. This crowding effect can bring change in subsequent chemical as well as signaling reactions [13]. Macromolecular crowding can be understood as a phenomenon that changes features like transport, diffusion, reaction, non-specific interaction, concentration, volume, pressure, viscosity and protein folding etc of the molecule in liquid state [12]. Heavily weighted or higher mass solutions like dextran or PEG are used here to provide a crowded environment on the lipid bilayer. The change in concentration of crowding agent changes the aggregation of proteins [14]. The crowding agents used for our

experiments just increases a viscous drag depending upon its concentration, but do not react with proteins or with each other.

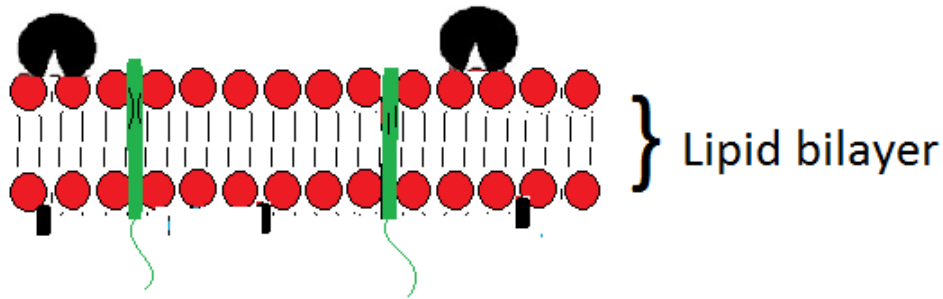


Figure 1.1: Components of crowded cell environment which has lipid bilayers, peripheral proteins, glyco proteins, transmembrane proteins etc. Proteins like C2 domains diffuse on these lipid membrane.

1.6 Fluorescence, microscopy and instruments

1.6.1 Total internal reflection fluorescence microscopy (TIRF)

Total internal reflection fluorescence (TIRF) microscopy is a technique that allows us to image our sample just near the cover slip providing better contrast and reduced background signal [16]. It is a useful method to understand mechanism in cell biology. Different range of lasers can be used for excitation of labeled molecules. The TIRF techniques work by illuminating the membrane layer just above the coverslip with an evanescent field created by excitation of laser passing by the coverslip with a large incident angle such that it can totally bounce back internally [17]. This incident angle must be higher than the critical angle. This illumination decays exponentially as increase in the distance normal to the surface, which has a capacity to excite the fluorophore in the sample [17]. The experiment included in this thesis is done on a home built total internal reflection microscope.

1.6.2 Fluorescence recovery after photo bleaching(FRAP)

Fluorescence recovery after photobleaching (FRAP) is a technique to understand the rate of diffusion [18]. In the FRAP technique we photobleach fluorescent molecules in a region

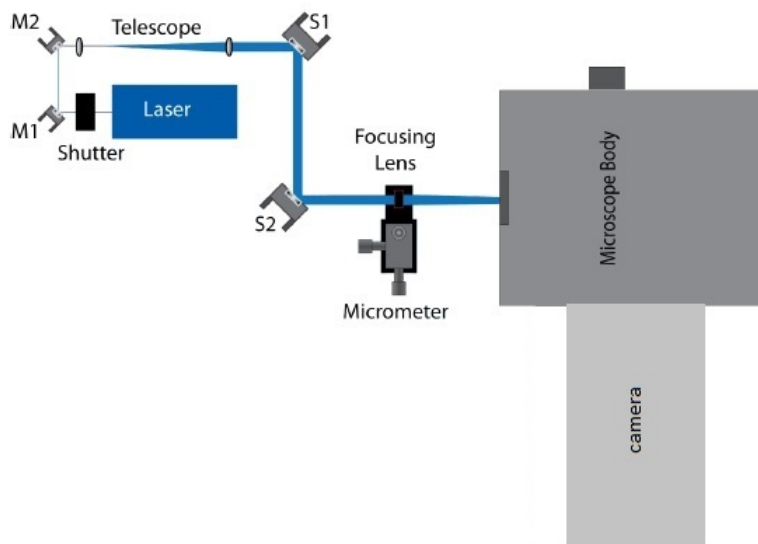


Figure 1.2: Schematic diagram of TIRF microscopy: This figure is taken from Aubrey Weigel’s dissertation [15]. The setup consists of telescope, mirrors, lenses, laser source (405 nm (violet), 473 nm (blue), and 532 nm (green), 561 nm (yellow), 638 nm (red)), aperture, focusing lens, microscope, objective, camera and shutters. Mirrors are navigating the laser beam. Telescope is used to expand the beam. Focusing lens is used for fine tune adjusting and focus beam on the back aperture of objective. Lasers 561 nm (yellow) and 473 nm (blue) are used for experiments in this thesis. Aperture is used to clean the beam size. Shutters are used to switch between lasers. Objective is used to magnify the imaging area. Camera records the movie/snapshots taken.

of interest (ROI) with a short but high intensity laser beam. Depending upon experimental requirements and applications along with advancement of technology, the ROI might be circular, rectangular and oval etc [16]. This intentional photobleaching process creates the concentration gradient of labeled molecules. Over time, the diffusion of molecules from neighboring areas of ROI into the photobleached area increases the concentration gradient of fluorescent molecules. Thus, during this time the previously photobleached area starts to recover its intensity. Imaging time of the experiment depends upon the amount of time needed for molecule intensity recovery. Change in average intensity of the ROI shows the rate of diffusion of molecules [19]. FRAP technique has been proven helpful to understand the diffusive properties of lipid bilayer membrane alone as well as with the crowding agents. The figure 1.3 (a-e) shows the process for performing FRAP.

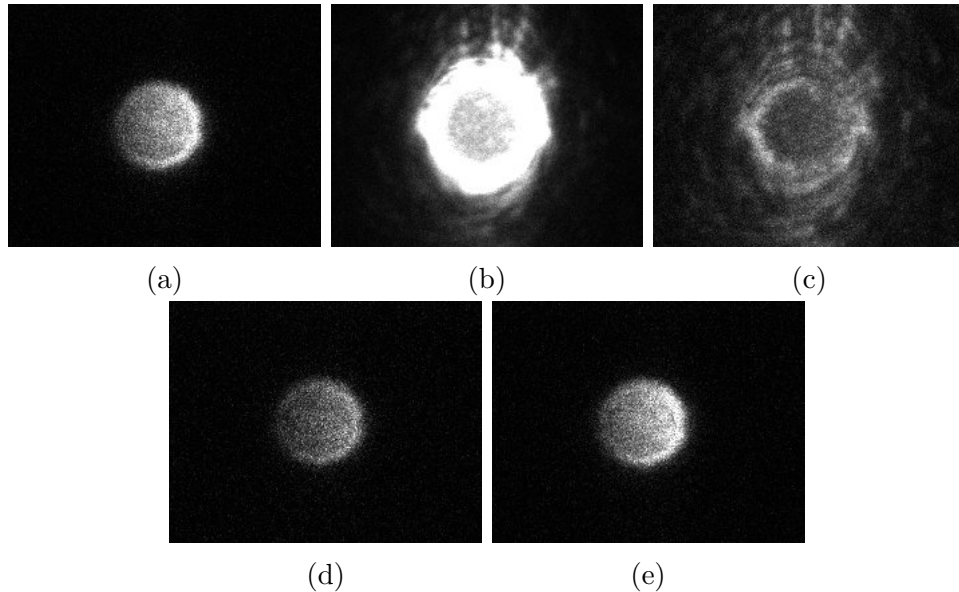


Figure 1.3: (a) Bright fluorescent sample before photobleaching, (b) Sample darkening while photobleaching, (c) Dark sample after photobleaching, (d) Sample when mid recovery, (e) Sample when fluorescence is recovered. Lipid bilayer is uniformly labeled with a fluorophore named fluorescein making them glow bright. Circular ROI on the sample is photobleached from high power laser which reduce the intensity to almost zero. The intensity within the same region of interest is monitored as the bleached lipid diffuses out and new lipid diffuses in during mid recovery. Over time the bleached ROI is recovered and the intensity is not increasing anymore.

1.6.3 Acoustic force spectroscopy (AFS)

The acoustic force spectroscopy (AFS) setup we used is manufactured by Lumicks. AFS technology utilizes acoustic waves to create a force on a glass flow cell to stretch beads attached to the nucleic acid [20]. The AFS setup can be used in bright field microscopy with water, oil or air objectives. The setup should have a wave function generator to provide oscillating voltage signals. The function generator is also used to get a resonant frequency to ultimately achieve the required acoustic wave force [20]. Two piezoelectric components are attached to the flow cell to generate force as shown in figure 1.4. These piezoelectric components vibrate to produce sound waves. The AFS setup in our lab applies force on the bottom surface of the flowcell to pull beads down. Mechanical experiments on single molecules can be successfully performed. For example biomolecules like DNA, RNA, Proteins can be duplicated, replicated [21], stretched, compressed, pulled, pushed, folded, unfolded [22] and repaired [21]. The acoustic wave force ranges of the AFS setup are wide enough to

perform single molecule experiments [20]. The results from the force application on beads attached to biomolecules can be observed in real time by looking at movement of the attached beads [20]. The accuracy for tracking the movement of beads is impressive.



Figure 1.4: AFS Acoustic Force Spectroscopy flow cell chip: There are two pairs of piezoelectric component with separate controls, one flow channel with inlet and outlet to do the experiment. Samples are bound on the surface of this channel.

1.7 Nucleic acid biology

1.7.1 DNA structure and function

The genetic information encodes for functional proteins that govern the processes in living cells. Nucleic acids are responsible for genetic information transfer in any living being. There are two broad types of nucleic acids. One type is deoxyribonucleic acid (DNA). In humans or any eukaryotic cells, DNA is found in nucleus but in bacteria or prokaryotic cells, DNA is found in cytoplasm. DNA is an organized polymer which plays a vital role in information transfer system. DNA has nucleotide named adenine (A), guanine (G), thymine (T) and cytosine(C). T is complement to A and C is complement to G meaning they bind to each other to form a double helix with hydrogen bond. The hydrogen bond can be torn apart by various factors like temperature, pH conditions, etc. [23]. DNA nucleotide has carbon sugar named deoxyribose, phosphate group and nitrogenous base. Each of three bases of a gene corresponds to a codon which eventually builds a protein chain. Phosphate groups bind one side on 3rd carbon atom of sugar and other side on 5th carbon of sugar to form a long chain of nucleotide with 5' and 3' end. The direction of DNA chain formation proceeds in 5' to 3'. Each base pair is 0.34 nm long and 2nm wide [24]. Entire central dogma deals with this transfer of genetic codes from DNA to RNA to proteins via methods called duplication, replication and transcription for gene expression.

1.7.2 RNA structure and function

RNA stands for ribonucleic acid. Like DNA, RNA also has its nucleotide with 5 carbon sugar (ribose). In comparison to features of DNA structure and function, RNA has Uracil (U) in place of Thymine (T). DNA provides a code to transcribe messenger RNA which expresses a protein. After transcribing messenger RNA (mRNA), this messenger RNA leaves the nucleus, goes to the cytoplasm and then goes to the ribosome. The ribosome translates the code along the mRNA to make protein sequence [25]. Like DNA, RNA has the capability to store genetic information on virus and does base pairing too. There is hydrogen bond between the two strands of RNA (dsRNA) but these bonds are stronger due to presence of additional OH group on ribose sugar. RNA structure is more stable as a double strand. The length of dsRNA are short compared dsDNA because dsRNA can form a 3 dimensional structure. The 3 dimensional structure of RNA is more complex than DNA which gives advantage for catalytic actions. The ribose on RNA has 2' hydroxyl [26].

MOTION OF MEMBRANE TARGETING C2 DOMAINS ON SYNTHETIC LIPID
BILAYER¹

2.1 Introduction

After arriving to plasma membrane, downstream signaling pathways are triggered by signaling molecules. Membrane targeting domains like C2 recruit these signaling molecules to the plasma membrane [28]. Synaptotagmin family of proteins plays an important role in vesicle docking and fusion during Ca^{2+} induced exocytosis in a wide variety of cell types. Synaptotagmin7 C2A binds to phospholipid components and is also sensitive to much lower concentrations of calcium. Its role as a calcium sensor derives primarily from its two C2 domains [29]. These domains are observed to have well characterized and has a long retention time on membrane. The regulatory domains or the amino-terminus of the Protein kinase C contains several shared sub regions: C2A domain is one of them [30]. C2 domains are regulatory sequence motifs that occur widely in nature. There are 125 human proteins that have C2 domains [31]. C2 domains were identified in a variety of proteins, including synaptotagmin. When C2 domains proteins binds to the membrane, this binding is not tight like we see in trans-membrane proteins where things bind and stay there for extremely long times. This docking on membranes is peripheral so they bind on one side of membrane. Because of this type of binding, after some time they come off the membrane. This transient association as well as dissociation nature of protein membrane interaction enables tight temporal regulations of signal transduction [27]. Molecules are also found to stay in its near neighborhood, diffuse, then jump far away. They are found to overcome the diffusion barriers in membrane. We can find this C2 domains appears in 125 different human pro-

¹Some sections of Methods, Material and Results are published in Nature - Scientific reports [27]. Link : <http://www.nature.com/articles/srep17721>. Grace Campagnola, Olve B. Peersen and Diego Krapf conceived the experiments. Olve B. Peersen and Diego Krapf supervised the project; Grace Campagnola prepared the samples, Kanti Nepal and Bryce W. Schroder conducted the experiments; Diego Krapf designed the analytical model and performed numerical simulations; Kanti Nepal and Diego Krapf analysed the results; Diego Krapf wrote the first draft.

teins [32]. There are numerous signaling proteins which by various mechanism are brought to cell membranes via phospholipids binding domains [33]. The idea is that this molecule will go and dock into the membrane and will perform 2D diffusion until they find specific target to trigger the downstream signaling pathway. They might activate or suppress the signaling pathways to eventually perform a biological process. These are molecules that are present in the cytoplasm of the cell. There are some conditions: like for C2 there is calcium signaling where C2 domains only binds to membranes in presence of calcium. They go and dock at the membrane and find some substrate that will modify the protein attached to it.

Some ideas about how common these things are, pleckstrin homology (PH) domains on supported lipid bilayers recognizes preinitiation complex (PIC) .This type of jumps are seen in PH domains and is attributed that these jumps happens as protein dissociates from lipid bilayer then does 3D diffusion and re-associates at another location rapidly in bulk solution [34]. 3D diffusion is supposed to be faster than diffusion at membrane because membrane is viscous environment compared to bulk. This type of motion is also observed in live cells. This was done for molecules called Phosphatase and tensin homolog (PTEN). PTEN is the molecule that inhibits growth of tumors. It is a cancer inhibitor. This also binds to membrane, does diffusion and perform jumps because of dissociation. Then it again rebinds to the membrane [35]. C2 domains regulates the PTEN membrane attraction [35]. This diffusion behavior was also observed in molecules at solid-liquid interfaces. Here it was done in absorption and disabsorption process of polymers at solid liquid interface [36]. Similarly it was seen in small molecules binding, unbinding and rebinding between solid and bulk liquid interface [37]. We can see in our experiment setup that C2 domains leave the 2D diffusive environment and does 3D long jump which yields anomalous diffusion and eventually affecting the target hunting process. This process where molecules alternate between 2D and 3D phase is bulk mediated diffusion. Nowadays, bulk mediated diffusion are being analyzed in many fields[22, 24].

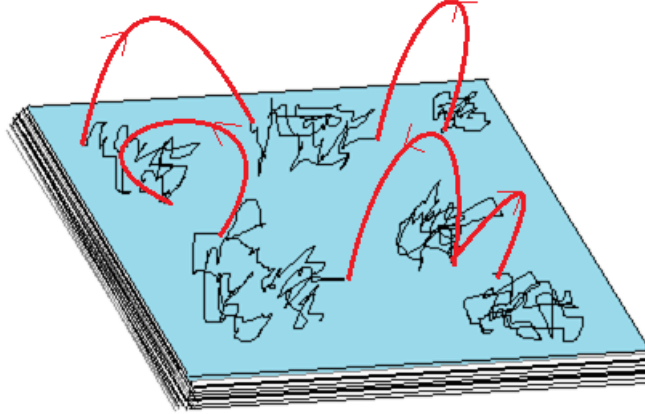


Figure 2.1: Molecule alternates between phases of two-dimensional and three-dimensional diffusion: Diffusion in the three-dimensional bulk is much faster than diffusion on the lipid bilayer, and thus only the effective two-dimensional process is observed without loss of trajectory connectivity. The excursions into the bulk are seen as long jumps in the two-dimensional trajectories.

2.2 Methods and materials

2.2.1 Sample preparation

Preparing protein

An expression plasmid containing the GST-ybbR-synaptotagmin7 C2A gene was transformed into *Escherichia coli* BL21- CodonPlus (DE3) competent cells. Cells were grown at 37°C to an OD_{600} of 0.6 and then induced to express protein with 0.5 mM IPTG for 6 hours at room temperature. The harvested cells were lysed at 18,000 lb/in² in a microfluidizer in a buffer containing 50 mM Tris, pH 7.5, and 400 mM NaCl, and centrifuged at 17,000 rpm in a Sorvall SS-34 rotor. The clarified lysate was loaded onto a 5 ml GSTrap FF column (GE Healthcare LifeSciences, Pittsburgh, PA) followed by gradient elution with 50 mM Tris, pH 8.0, 100 mM NaCl, and 10 mM glutathione. Fractions containing protein were pooled and diluted to reduce the salt to less than 0.1 M prior to loading onto a HiTrap Q HP column (GE Healthcare LifeSciences) and eluting with a linear gradient to 1 M NaCl in 25 mM Tris, pH 8.5, 20% (v/v) glycerol, and 0.02% (w/v) NaN₃. A portion of the purified protein was subjected to thrombin cleavage to remove the GST tag and then separated using a Superdex 200 gel filtration column (GE Healthcare LifeSciences) equilibrated in 50 mM Tris, pH 7.5,

and 100 mM NaCl. 20 mM CoASH (New England Biolabs, Ipswich, MA) in 400 mM Tris, pH 7.5, was mixed with 20 mM ATTO-565 maleimide (ATTO-TEC, Siegen, Germany) in dimethylformamide and incubated at 30°C overnight to form ATTO-565 CoA, then diluted 10-fold with 5 mM DTT and 10 mM Tris, pH 7.5, to quench the reaction. ybbR-Syt7 C2A was labeled with ATTO-565 via SFP synthase (40-phosphopantetheinyl transferase). Samples were dialyzed against 1 L of 50 mM HEPES, pH 7.0, 75 mM NaCl, 4 mM MgCl₂ and 5% glycerol overnight at 4°C and then concentrated to 10 mM.

Supported lipid bilayer construction

Phospholipids were purchased from Avanti Polar Lipids (Alabaster, AL). Chloroform-suspended 18:1 (Δ 9-Cis) PC (DOPC) and 18:1 PS (DOPS) were mixed at a ratio of 3:1. The phospholipid mixture was vacuum dried overnight and resuspended in imaging buffer (50 mM HEPES, 75 mM NaCl, 1 mM MgCl₂, 2 mM tris (2-carboxyethyl) phosphine (TCEP), and 200 mM CaCl₂) to a final concentration of 3 mM followed by probe sonication to form sonicated unilamellar vesicles (SUVs) [38]. A solution of SUVs (1.5 mM lipid) in 0.5 M NaCl and imaging buffer was introduced into a perfusion chamber (CoverWell, Grace Bio-Labs model PC8R-1.0) and incubated for one hour at 4°C. The surface was then rinsed with imaging buffer multiple times prior to the addition of the protein sample.

Selection of surface environment

Glass coverslips were cleaned by sonication in a detergent solution followed by soaking in 1 M KOH. The coverslips were rinsed extensively in Milli-Q water and blown dry with a stream of nitrogen gas. Then, the coverslips were treated with an oxygen plasma. Immediately after the plasma cleaning, a perfusion chamber (CoverWell, Grace Bio-Labs model PC8R-1.0) was adhered to the coverslip.

2.2.2 Instrumentation and software

Imaging setup

Proteins were added to the imaging buffer to a final concentration of 75 pM. Then, the perfusion chamber was filled with the solution. The perfusion chambers were 9 mm in diameter and 0.9 mm deep, holding a volume of 60 μ l. Imaging was performed at room temperature without replacing the solution, so that there was always protein present in the bulk solution and the surface concentration could reach a steady state. All images were acquired using an objective-type total internal reflection fluorescence microscope (TIRFM) [16] [17]. The microscope was home-built around an Olympus IX71 body [39] [40] with a 561 nm laser line as excitation source. A back-illuminated electron-multiplied charge coupled device (EMCCD) camera (Andor iXon DU-888) liquid-cooled to -85°C , with an electronic gain of 300 was used. In order to maintain constant focus during the whole imaging time we employed an autofocus system (CRISP, Applied Scientific Instrumentation, Eugene, OR) in combination with a piezoelectric stage (Z-100, Mad City Labs, Madison, WI). Videos were acquired at a frame rate of 20 frames/sec. using Andor IQ 2.3 software and saved as 16-bit TIFF files. The images were filtered using a Gaussian kernel with a standard deviation of 1.0 pixel in ImageJ. Single-particle tracking of ATTO-C2 was performed in MATLAB using the u-track algorithm developed by Jaqaman et al [41].

Building chamber with samples

Perfusion chamber (CoverWell, Grace Bio-Labs model PC8R-1.0) used in this experiment has one inlet and another outlet hole as shown in figure 2.2 below. The lipids, buffers, proteins are squirted into the perfusion chamber from one hole. The sample inside the chamber is found to remain stable throughout the experiment but gradual drying has occurred. We have protected the sample from drying by squirted 5-10 μ l extra than chamber's volume capacity. The chamber's volume is 60 μ l.

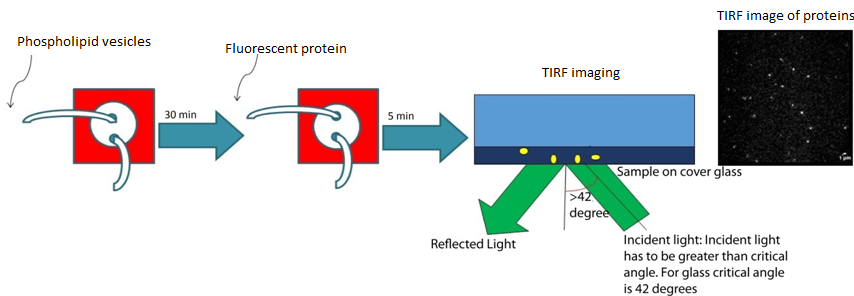


Figure 2.2: Steps to perform the experiment for chapter 2. The red square structure is the schematic for chamber well with two holes (inlet and outlet). There are tubes connected to each holes. The TIRF imaging schematic shows how this imaging techniques work. The example frame shows how the molecules look like while recording. Incubation times might vary depending upon the density of molecules in one field of view.

2.3 Results

Some portion of this section and pictures are taken from the paper Superdiffusive motion of membrane- targeting C2 domains. My advisor Diego Krapf wrote the manuscript. I am co-author and individual roles are clarified [27]. We have supported lipid bilayer constructed with 3:1 ratio of phosphatidylcholine (PC) and phosphatidylserine (PS). Next we have membrane targeting C2A domains from synaptotagmin 7 [42]. To understand the diffusion behavior of this C2A domains proteins we used single molecule measurement technique. Each C2A domains proteins were tagged with ATTO- 565 and yellow (561 nm) laser was used to image them. Glass coverslip with a chamber well was used to assemble the lipid bilayer and were imaged by total internal reflection microscopy. The concentration of proteins were understood by the amount of fluorescent molecule we saw on one imaging window meaning that the density it covered on one field of view. We tried to avoid any mis-connections, collisions so that diffusion tracking is not interrupted even after long jumps. The frame rate at which our movies were taken is 20 frames/ second.

Figure 2.3 (a) shows trajectories obtained in a 10-s window, overlaid on the last frame. Figure 2.3 (b,c) shows that the protein jumped from surface- readsorb on liquid bulk then made a jump through this bulk which is seen as reduced intensity in previous and later location in the same frame. Diffusion in bulk is 100 times faster than that of surface [43].

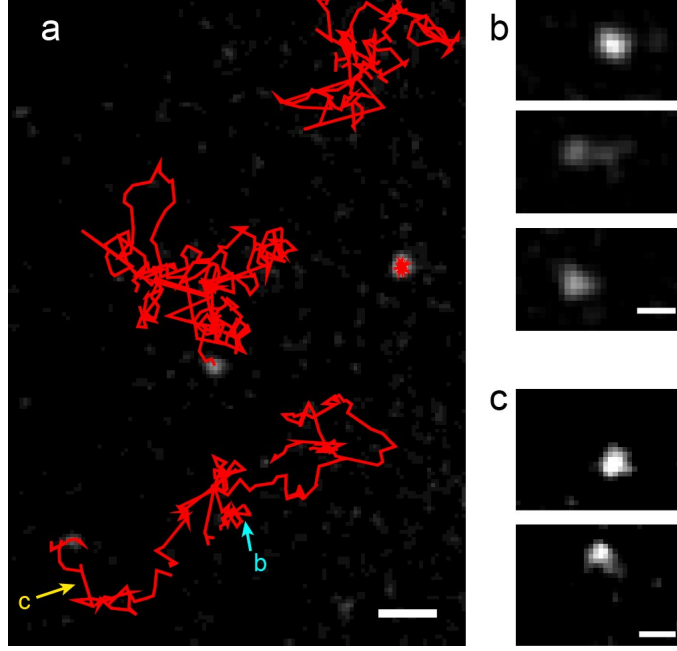


Figure 2.3: (a) C2A-ATTO 565 individual trajectories collected during a 10-s time window. Three mobile trajectories are observed in the image together with one immobile particle that is tracked but is not included in the analysis. The last frame is overlaid on the trajectories. Scale bar $2 \mu\text{m}$. (b) Region of interest (ROI) around the location of a micrometer jump that occurs in the lowermost trajectory, marked with the letter b. Three frames are shown corresponding to before, during, and after the jump. Scale bar $0.5 \mu\text{m}$. (c) ROI around the location of the jump marked with the letter c. Scale bar $1 \mu\text{m}$.

To have a control experiment we fused C2A domains with GST (glutathione S-transferase) to make a dimer as shown in figure 2.4 (a). Different dissociation constant was observed because this dimer has two types of interaction with the membrane and increased viscous drag coefficient which eventually slows down the dissociation rate and diffusion coefficient to almost half. 14,000 C2A and 3600 C2A-GST mobile trajectories were collected excluding the immobile molecules. Single displacement from each trajectory is taken to find ensemble-averaged MSD $\langle r^2(t) \rangle$ which is not linear and shows superdiffusive behavior as shown in figure 2.4 (b). Onset of superdiffusion for C2A-GST dimer occurs at a later time than C2A alone. The time-averaged MSD $\overline{\delta^2(\Delta)}$ is used in the analysis of individual trajectories.

$$\overline{\delta^2(\Delta)} = \frac{1}{N-n} \sum_{j=1}^{N-n} [r(j\tau + \Delta) - r(j\tau)]^2 \quad (2.1)$$

where, τ is the time interval between consecutive measurements, $n = \frac{\Delta}{\tau}$ and N is the time

points for equation above. Figure 2.4 (c) shows the time-averaged MSD after it is additionally averaged over all the trajectories. C2A-GST has slower diffusion rate than C2A, based on the MSD slope. For ergodic processes, the temporal and ensemble averages coincide in the long time limit $\overline{\delta^2(\Delta)} = \langle r^2(\Delta) \rangle$. However, the ergodic hypothesis breaks down for C2A molecules. In contrast to the ensemble-averaged MSD, the time-averaged MSD is linear in lag time.

$$\overline{\delta^2(\Delta)} \sim \Delta \quad (2.2)$$

So, while analyzing time-averages can lead us to conclude that the diffusion is not anomalous. The distribution of displacements $P(r)$ at $\Delta = 100$ ms is shown in Figure 2.4 (d,e) for C2A and GST-C2A respectively. The distribution exhibits two characteristic regimes: a central part up to a distance $r \approx 1.5$ m and a long tail. This behavior can be understood from the scaling properties of bulk-mediated diffusion as discussed by Bychuk and O Shaughnessy [44]. Once a molecule dissociates from the surface, it performs a three-dimensional random walk until it returns. In the asymptotic limit, the first return time distribution scales as $\psi(\tau) \sim \tau^{-1.5}$. For any given return time, the surface distance between the dissociation and return points has a Gaussian distribution $P(r_j | \tau) \sim \exp(-r_j^2/4D_b\tau)$. Therefore, the distribution of jump lengths is $P(r_j) \sim r_j^{-3}$, as observed in Figure 2.4 (d,e) for long distances. The theoretical probability density function of jump lengths can be found using the image method [45]. The distance of first return to the surface are governed by $P(r) = \gamma_o/2\pi(r^2 + \gamma_o^2)^{3/2}$ that is a two-dimensional Cauchy distribution. At short times, the probability that the particle performs more than a single jump is small. If we neglect the distance covered by surface diffusion within time intervals at which the particle undergoes a bulk excursion, the motion at each short interval is either by surface diffusion or via a jump. We can then approximate the distribution of displacements at short times by

$$P(r) = w \frac{\gamma_0}{2\pi(r^2 + \gamma_0^2)^{3/2}} + \frac{1-w}{2\pi\sigma^2} \exp\left(\frac{-r^2}{2\sigma^2}\right) \quad (2.3)$$

where w is the probability that the particle hops within the given time and surface diffusion yields $\sigma^2=2D_s t$. A least-square fitting of the distribution of displacements as shown

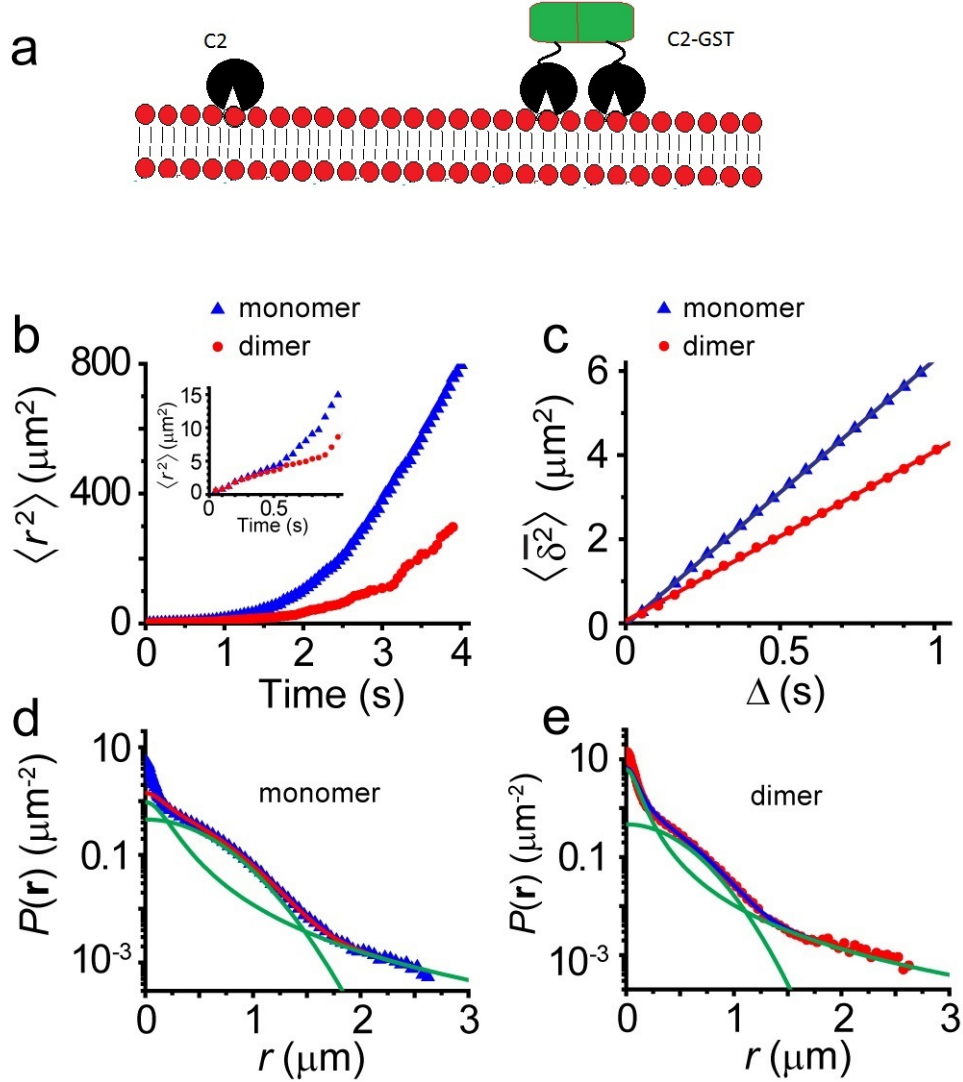


Figure 2.4: Anomalous diffusion analysis of membrane-targeting domains C2A (monomer) and dimer forming GST-C2A. (a) Sketch of the C2A monomer and the GST-C2A dimer employed in this study. (b) Ensemble-averaged MSD $\langle r^2(t) \rangle$. The inset provides a zoom of the data so that it is presented with the same time axis as the time-averaged MSD, for comparison. (c) Time averaged MSD as a function of lag time Δ . The time-averaged MSD of individual trajectories varies greatly, so the MSDs of individual trajectories are also ensemble averaged. (d,e) Distribution of displacements for $\Delta = 100$ ms. The total number of displacements are 207,000 and 56,000 for C2A and GST-C2A, respectively. The solid lines show fitting to equation (4) [TODO] and to the individual components of the propagator, i.e. the Gaussian part $\frac{1-w}{2\pi\sigma^2} \exp\left(-\frac{r^2}{2\sigma^2}\right)$ and the Cauchy propagator part $w \frac{\gamma_0}{2\pi(r^2+\gamma_0^2)^{3/2}}$. The cutoff at $2.6 \mu\text{m}$ appears because trajectories are not connected when jumps longer than this distance take place. This threshold is placed in order to avoid the risk of particle misconnections.

in Figure 2.4 (d,e) to this propagator yields $D_s=1.7 \mu\text{m}^2/\text{s}$ for C2A monomers and $D_s=1.0 \mu\text{m}^2/\text{s}$ for GST-C2A dimers. The parameter γ is found to be $0.24 \mu\text{m}$ and $0.12 \mu\text{m}$ for C2A and GST-C2A, respectively. The distribution of displacements for longer times involves both a random number of jumps, each having a Cauchy distribution, and the Brownian motion on the surface. Chechkin et al. derived the full solution for the propagator of bulk-mediated diffusion [46]. For the case when $D_s=0$ and neglecting long distance corrections, the distribution of displacements is given by the Cauchy propagator, in agreement with scaling arguments [44],

$$P(r) = \frac{\gamma t}{2\pi[r^2 + (\gamma t)^2]^{3/2}} \quad (2.4)$$

When the particles also diffuse on the surface, i.e. $D_s \neq 0$ the probability density of the displacements is given by the convolution of equation above with a normal distribution. Even though the full solution for long times is complicated, the tail of this distribution for large distances still scales as $P(r) \sim r^{-3}$. Due to this asymptotic behavior, the exact distribution has similar properties to the Cauchy distribution.

2.4 Discussion and conclusion

C2 domains molecules derived from synaptotagmin 7 are labeled with ATTO 565 fluorophore. Our experimental samples also had C2 fused to GST(glutathione S-transferase), a dimer for control purpose. The C2-GST binds double the amount of lipid head groups comparative to C2 alone doubling the frictional and drag effects slowing down its diffusion. C2 domains is a 116 amino acid sequence which binds to lipid head groups phosphatidylserine (PS) in the membrane when calcium is available [29] [47]. Our experiment was done on synthetic lipid bilayer with chamber well stuck to the coverslip giving us freedom to decide on factors like buffers,salts, lipid content, shape of the lipids [48]. Our model membranes provide an excellent environment to study the effect of superdiffusive Lévy flights because our model system is controlled and protected from other activities that would normally happen in real time. We tried to create a replica of native environment as that would be in-vivo [49] for our membrane targeting protein but at the same time we also isolated it

alone to avoid the unwanted affect. We used total internal reflection fluorescence (TIRF) microscopy because TIRF imaging system allows us to image sample just above the coverslips precisely with 100 nm range and eliminating the background. After imaging, the movies recorded are analyzed by tracking the fluorescent molecules when they diffuse on our synthetic lipid bilayers to find the diffusion coefficients and protein lipid interactions. Lèvy flights described our protein diffusion where we have a random walk with steps displacements having heavy tailed distribution. When our proteins dissociates spontaneously from lipid membrane it does 3D random walk before they find back the surface. This 3D diffusion is responsible for the heavy tail distribution. The propagator for surface diffusion in the presence of bulk-mediated jumps depends on the surface diffusion coefficient and the transition between membrane surface and bulk phase which is explained by the parameter γ . We get $\gamma \sim \alpha/\tau_{des}$ where τ_{des} is the mean desorption time and α is a dimensional factor. Bulk-mediated diffusion thus predicts $\gamma_{dimer} < \gamma_{monomer}$, in agreement with the values we find for C2A and GST-C2A. In our results we have normal diffusion behavior from time averaged MSD and superdiffusion behavior from ensemble average MSD which shows weak ergodicity breaking in the process [50]. In our experiments we have not excluded the effect of long bulk mediated jumps like that done in literature [45] [47]. Effective search of target to bind leads to this motion as described by Lèvy flight with jumps to give a heavy tail distribution which are caused by excursion into liquid bulk where diffusion is much faster.

INFLUENCE OF CROWDING AGENT ON LIPID BILAYERS IN PRESENCE AND
ABSENCE OF PROTEINS²

3.1 Introduction

The cell membrane is a key component of a cell which is a communication platform for inside and outside of the cell. It functions as tightly regulated fence which protects delicate components in the cell [51]. The cell membrane is a busy environment because it has a diverse set of membrane proteins like trans-membrane proteins, peripheral proteins, membrane targeting domains, glyco proteins as well as underlying cytoskeleton. The lipid bilayer is the key component of the cell membrane. Lipid bilayer is also formed from large variety of lipids [52]. Similar to chapter 2, we have phosphatidylcholine (PC) and phosphatidylserine (PS) at 3:1 ratio to make a lipid bilayer. Building upon the research presented in chapter 2, the focus of chapter 3 shifts to explain the effect of crowding agents on bulk-mediated diffusion of membrane targeting C2 domains. Similar to chapter 2, C2 domains proteins were labeled with ATTO 565. As a control experiment, a fluidity check was also performed on lipids labeled with the fluorescein. Crowding agent, Polyethylene glycol (PEG) is a vital viscosity enhancing tool used to simulate a busy cellular environment in vitro. PEG molecule is non-toxic unique polymer with the chemical structure $\text{HO}(\text{CH}_2\text{CH}_2\text{O})_n\text{H}$ [53]. PEG molecules are water soluble. This water solubility comes from hydrophilic heads made up of hydroxyl groups. PEG can also be dissolved in most of the organic solvents [54]. This solubility comes from the presence of polyoxyethylene chain. The PEG molecules are also biologically inert, non-immunogenic and highly flexible to provide surface treatment. Because of the easy availability and unique properties of PEG, it is commonly used in such biomedical

²Some sections of results, methods and materials are from paper published in Nature- Scientific reports because experiments on this chapter are the continuation from chapter 2. Link : <http://www.nature.com/articles/srep17721>. For these set of experiments credits are : Grace Campagnola, Olve B. Peersen and Diego Krapf conceived the experiments. Olve B. Peersen and Diego Krapf supervised the project; Grace Campagnola and Kanti Nepal conducted the experiments. Data analysis for experiments with crowding agent on C2 domains were analyzed by Kanti Nepal. Data analysis for experiments with crowding agent on fluorescent lipids were analyzed by Kanti Nepal and Grace Campagnola.

research as surface functionalization, tissue scaffolds and many more [55]. PEG is found in wide range of oligomer sizes defined as molecular weights. For our experiment, we chose to use PEG 3350. PEG crowding affects solute diffusion and causes segregation of molecules. This effect is size and concentration dependent, meaning that the size and concentration of PEG determines the change in diffusion behavior [56]. We observed anomalous behavior (superdiffusive) of membrane targeting C2 domains in chapter 2. Anomalous behavior has been seen in living cells [57]. The anomalous diffusion behavior alters the outcome of the search processes as well as the upcoming molecular reactions. The diffusion becomes anomalous, meaning that there is no linear relationship between mean square displacements and time anymore. Instead the mean square displacement (MSD) scales as a power law with an exponent $\alpha \neq 1$ [58].

$$P(r) = \langle x^2(t) \rangle = K_\alpha t^\alpha \tag{3.1}$$

where K_α is the generalized diffusion coefficient with units cm^2/s^α . When $\alpha < 1$, the process is subdiffusive, and when $\alpha > 1$, it is superdiffusive. The crowding causes subdiffusion [59]. In this chapter, we report the experimental observation of sub diffusion transport of membrane targeting C2 domains on supported lipid bilayers. Literature shows that when high concentration of macromolecules (PEG) is in a restricted environment, the dense characteristic of these macromolecules happen to be one of the determining factors for the thermodynamic change of that environment [60] [61]. This dense character of macromolecules plays a vital role in the diffusion of molecules depending upon the concentration, size and shape of crowding agent [60]. Crowding agents like PEG are known to physically decrease the diffusion of molecules [61] causing their mean squared displacements to have a non-linear relation with time [12]. However this behavior is protein dependent meaning that different proteins might show different diffusion behavior to the same crowding agent. This set of experiment deals with C2 domains proteins as diffusing molecules and PEG as crowding agent.

3.2 Methods and materials

3.2.1 Sample preparation

Preparing protein

Protein preparation is explained in the methods and materials section of chapter 2. All protocols were kept consistent in this set of experiments because our goal was to understand the effect of the crowding agent on the same supported lipid bilayer with same the membrane targeting C2 domains proteins. The only difference in this section is that we did not perform the C2-GST control experiment.

Supported lipid bilayer construction

Supported lipid bilayer construction is also explained in methods and materials of chapter 2. All protocols were kept consistent in this set of experiments because our goal was to understand the effect of crowding agent on the same supported lipid bilayer with the same membrane targeting protein C2 domains. There is absolutely no change in the protocols for constructing the supported lipid bilayer in chapter 3 as described in chapter 2.

Selection of surface environment

Selection of surface environment is also explained in methods and materials of chapter 2. All protocols were kept consistent in this set of experiments because our goal was to understand the effect of crowding agent on the same supported lipid bilayer with the same membrane targeting protein C2 domains. There is absolutely no change in the protocols for constructing the supported lipid bilayer in chapter 3 as described in chapter 2.

3.2.2 Instrumentation and software

Imaging setup

Imaging setup is also explained in methods and materials of chapter 2. All protocols were kept consistent in this set of experiments because our goal was to understand the effect

of crowding agent on the same supported lipid bilayer with the same membrane targeting protein C2 domains. In addition to understanding the change in motion of C2 domains, we also looked at diffusion of lipids by Fluorescence recovery after photo bleaching (FRAP) technique. The FRAP experiment was done by fixing the aperture size for photo bleaching. The imaging setup was all consistent except for the aperture and imaging time. Before photo bleaching, we recorded for 40 seconds with an interval of 10 seconds at frame rate of 1 frame per second with 30 ms exposure. Then we photo-bleached continuously with a high power laser for 6 seconds at frame rate of 1 frame per second with 30 ms exposure. The recovery was recorded for 800 seconds with interval of 2 seconds at frame rate of 1 frame per second with 30 ms exposure. The intensity within that aperture area was analyzed by using ImageJ to understand the recovery of the fluorescent lipids.

Building chamber with samples

Building chamber with samples is also explained in methods and materials of chapter 2. All protocols were kept consistent in this set of experiments because our goal was to understand the effect of crowding agent on the same supported lipid bilayer with the same membrane targeting protein C2 domains. There is absolutely no change in the protocols for constructing the supported lipid bilayer in chapter 3 as described in chapter 2.

Preparing series of PEG concentration

PEG with molecular weight 3350 was used for this experiment. Initially, 50% (w/v) PEG from the powder was made. This solution was made to prepare a series of 37.5% (w/v), 25% (w/v), 20% (w/v), 15% (w/v), 10% (w/v), 0% (w/v) in buffer. Detailed protocol to make this series is explained in Appendix A.7.

Preparing fluorescent lipid

The lipid, phosphatidylethanolamine (PE) was fluorescently labeled for FRAP experiment. The stock concentration was 880 μM fluorophore assuming that purification is done in such a way that it is one to one ratio with lipid during purchase meaning 880 μM of fluorophore

with 880 μM of lipids. For our set of experiments, total concentration of lipids has to be 3 mM. After conducting several experiments, conclusion was made that we need 1% of our 3 mM i.e 30 μM fluorescent lipids for good coverage. This experiment needs a lipid bilayer. The Lipids had to be dried overnight in vacuum centrifuge to get rid of all the chloroform that comes while purchase because while chloroform is good at keeping lipids monomeric and clear during purchase and transport it is not good for bilayer formation. When we dry lipids and re suspend it again it is cloudy. We need to sonicate it to break it into monomers and make it clear. Detailed protocol is explained in Appendix A.3 and A.9.

3.3 Results and discussion

3.3.1 Effect of PEG on C2 domains

After video-microscopy, the saved movies are filtered and processed with ImageJ. The image is thresholded and convoluted with a Gaussian function with the standard deviation sigma of 1 to improve signal to noise ratio, eliminate background noise and to eliminate speckling. Matlab tracking software U-Track is used to get individual trajectories for individual molecules [41]. U-Track finds the location of each molecule in the form of x, y co-ordinates along with intensity of each molecules in each frame. These locations of molecules are converted from pixels to nm units. Along with the pixel to nm conversion process, it also gives the length of each trajectories formed by each molecules. The U-Track software detects the center locations of each molecules. The trajectories formed by these molecules are used to find the mean squared displacements (MSD) and diffusion coefficients. MSD is observing how fast and how far particles move by tracking positions of particles at specific number of frames. For example, If we have to find displacements through 5 frames then we are looking at displacements between frame 1 and 6, 2 and 7 and so on. This value (5 frames) is called lag time where lag time is calculated by $tlag = \frac{movieduration}{Totalnumberofframes}$. For our experiments, movie duration was 30 seconds and number of frames was 580 which gave 1 lag time as 50 ms. After MSD, the time averaged mean square displacement (TAMSD) is calculated. TAMSD is calculated for one trajectory. We averaged squared displacements for one particle that happens for a specific lag time. For (TAMSD), we have time series t_1, t_2, \dots, t_{N-1} ,

t_N . Lag time is denoted here as Δ . For example, if Δ is 50 ms, we calculate displacements from frame 1 to frame 2 to frame 3 ($t_1 \rightarrow t_2 \rightarrow t_3$) and so on. This displacement is called ΔX for $\Delta = 1$.i.e. 50 ms. To calculate TAMSD we used formula $\sum_{i=1}^N \frac{\Delta X_i(\Delta=1)}{N}$ where ΔX_i is the displacement, Δ is lag time and N is the total number of frames of that track. Like shown in chapter 2, figure 2.4 (c), TAMSD is additionally averaged over all trajectories so that we can eliminate the large scattering between different trajectories. The number of trajectories might be more than the number of molecules because one single molecule can lose a trajectory at some point and start a new trajectory again. After calculating TAMSD, we calculate diffusion coefficients (D) which results in format of 3 columns: slope, residual and intercept respectively. As shown in equation 3.2 the diffusion coefficients are calculated by averaging the the slopes of TAMSD after it is divided by 4. Intercept is where the slope meets on the y-axis. Residual is the value for how close our data is to the averaged slope. The smaller the residual value, the better the averaged slope fit.

$$\langle r^2 \rangle = 4D\Delta t \quad (3.2)$$

Next step is calculating displacements. For our experiments, we calculated displacements with a lag time of 2 meaning that the distribution of displacements $P(r)$ is at $\Delta = 100$ ms. Similar to chapter 2 and as shown in equation 3.3, distributions of displacements for short times is modeled with a propagator that includes contributions from Gaussian surface diffusion and a Cauchy distribution due to bulk excursions. The distribution shows evidence of two characteristic regimes: a central part and a long tail. The surface motion of these membrane-targeting domains is well described by Lèvy flights, a random walk where the step displacements have a heavy-tailed distribution. Therefore, the heavy tail arose from the dissociation of molecules from the membrane, and then the molecule performed a three-dimensional random walk until they reach the surface again at another location.

The surface distances covered by jumps had a Cauchy distribution, which was responsible for the heavy tail in the Lèvy flights. The tail in the MSD distribution of C2 domains decreased faster. This effect was caused by an artificial truncation of the distribution of

displacements caused by the tracking algorithm [27]. If a particle experiences a long jump, it is not possible to make frame-to-frame connections with reasonable confidence and thus trajectories are cropped, missing the long displacements and in turn the large diffusivities. The distance of first return to the surface is governed by $P(r) = \gamma_0/2\pi(r^2 + \gamma_0^2)^{3/2}$ that is a two-dimensional Cauchy distribution. We can then approximate the distribution of displacements at short times by

$$P(r) = w \frac{\gamma_0}{2\pi(r^2 + \gamma_0^2)^{3/2}} + \frac{1-w}{2\pi\sigma^2} \exp\left(\frac{-r^2}{2\sigma^2}\right) \quad (3.3)$$

We get the diverging second moment in this propagator from equation 3.3 implying that there is a non-negligible probability for the occurrence of extremely long jumps. This phenomenon has direct implications in the measured MSD.

Experimental results of membrane-targeting C2 domains on supported lipid bilayers in presence of crowding agent PEG reported a strong shift in distribution of diffusion coefficient as presented in figure 3.2 (a-f). This figure shows that there is a shift in peak diffusion coefficients as PEG percentage increases. The overall diffusion coefficients decreased with respect to increasing PEG percentage w/v. Parameter γ reflects the transition between the surface and the bulk phase. γ also corresponds to bindings. γ decreased with increase in PEG concentration as shown in figure 3.3 (b). The trend in γ values were: $0.38 \mu\text{m} > 0.29 \mu\text{m} > 0.23 \mu\text{m} > 0.2 \mu\text{m} > 0.1 \mu\text{m} > 0.07 \mu\text{m}$ with respect to 0% w/v , 10% w/v, 15% w/v, 20% w/v, 25% w/v, 37.5% w/v of PEG. Our experimental results also reported a strong trend in mean desorption time τ_{des} as shown in figure 3.3 (d). Mean desorption time is calculated by $\tau_{des} = 1/\text{gamma}$ with arbitrary units. Gamma is inversely proportional to desorption time. As gamma goes down desorption time goes up.

The trend in τ_{des} values were: $2.63158 > 3.44828 > 4.34783 > 5 > 10 > 14.28575$ with respect to 0% w/v , 10% w/v, 15% w/v, 20% w/v, 25% w/v, 37.5% w/v of PEG. Jump population and desorption time τ_{des} are increasing with increasing PEG percentage w/v because molecules do not move long distances during diffusion. So, more population are seen with longer jumps. Another strong trend was seen in parameter ω as shown in figure

3.3 (a) where ω is the probability that the particle hops within the given time. ω is also the approximation that there is a single jump. It indicates what population of molecules spends how much time in surface versus bulk. The trend in ω values were: $0.09091 > 0.16667 > 0.2 > 0.21875 > 0.33 > 0.65217$ with respect to 0% w/v, 10% w/v, 15% w/v, 20% w/v, 25% w/v, 37.5% w/v of PEG. The trend of ω in this experiment was counter intuitive. One reason for this increasing trend of ω might be that overall amount of time spent jumping is larger as PEG percentage increases. It was expected that ω would decrease but in our experiment it increased. It was also expected that the molecules would not jump because of the pressure created by crowding agent. In contrast to what was expected, we saw that molecules managed to jump and once they jumped they had more difficulty coming back making them more prone to jump. Another possibility might be that the tendency to spend more time in the bulk increases when longer jumps are happening more than shorter ones. If a molecule manages to jump, then it takes much more time to come back which might be the reason we start to see more jumps as concentration of PEG increases. Therefore, counter intuitively long jumps have higher probability as concentration of PEG increases.

Here, we did not just have 2 population of molecules: diffusing and jumping. We also had a fraction of molecules that were immobile. This immobile population was more prominent when we had crowding involved in PEG experiments. ω here is the fraction of molecules that jumped but this fraction was not out of total population. It was the fraction without including the immobile population. If we included the total population this fraction would not change but would have changed if we included the immobile part. Because the immobile part was taken out of population that was diffusing but not jumping. Another parameter shown in figure 3.2 (c) is σ whose distribution did not follow any sort of increasing or decreasing trend up until 20%. The decreasing trend of σ started after 25% PEG w/v. σ is the estimation of surface diffusion. The trend in sigma: $0.47 > 0.47 > 0.47 > 0.45 > 0.4 > 0.36$. The last parameter is the trend in immobile population. It is the percentage of population of molecules that had less than 280 nm displacement. The trend in immobile population was: $11\% > 18\% > 25\% > 29\% > 40\% > 54\%$ with respect to 0% w/v, 10% w/v, 15% w/v, 20% w/v, 25% w/v, 37.5% w/v of PEG. The trend of immobile molecules

strongly showed that as concentration of PEG increased, the immobile population percentage increased respectively.

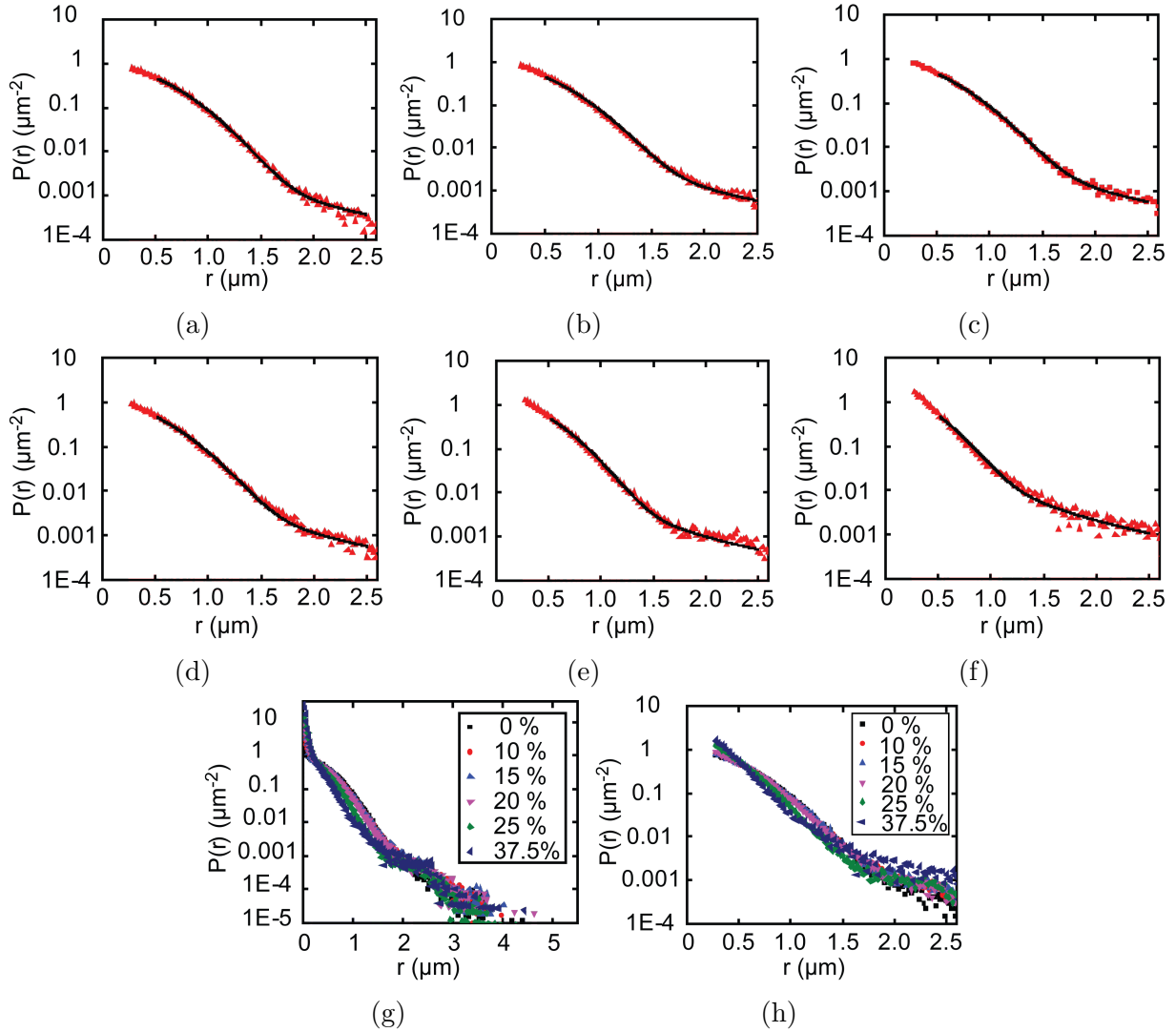


Figure 3.1: Distribution of displacements. (a) 0% PEG w/v, (b) 10% PEG w/v, (c) 15% PEG w/v, (d) 20% PEG w/v, (e) 25% PEG w/v, (f) 37.5% PEG w/v, (g) all% of PEG w/v, (h) all% of PEG w/v from 280 nm. Figure (a)–(f) are distribution of displacements for $\Delta = 100$ ms. Figure(g) is the total (mobile+ immobile) distribution of displacements. Figure(h) is the distribution of displacements without including the displacement less than 280 nm. Solid black lines show fit to equation 3.3 which has Gaussian part $\frac{1-w}{2\pi\sigma^2} \exp(-\frac{r^2}{2\sigma^2})$ and Cauchy propagator part $w \frac{\gamma_0}{2\pi(r^2+\gamma_0^2)^{3/2}}$. Similar to chapter 2, cutoff is at $2.6 \mu\text{m}$ because trajectories are not connected when jumps longer than this distance take place. This threshold is placed in order to avoid risk of particle mis-connections.

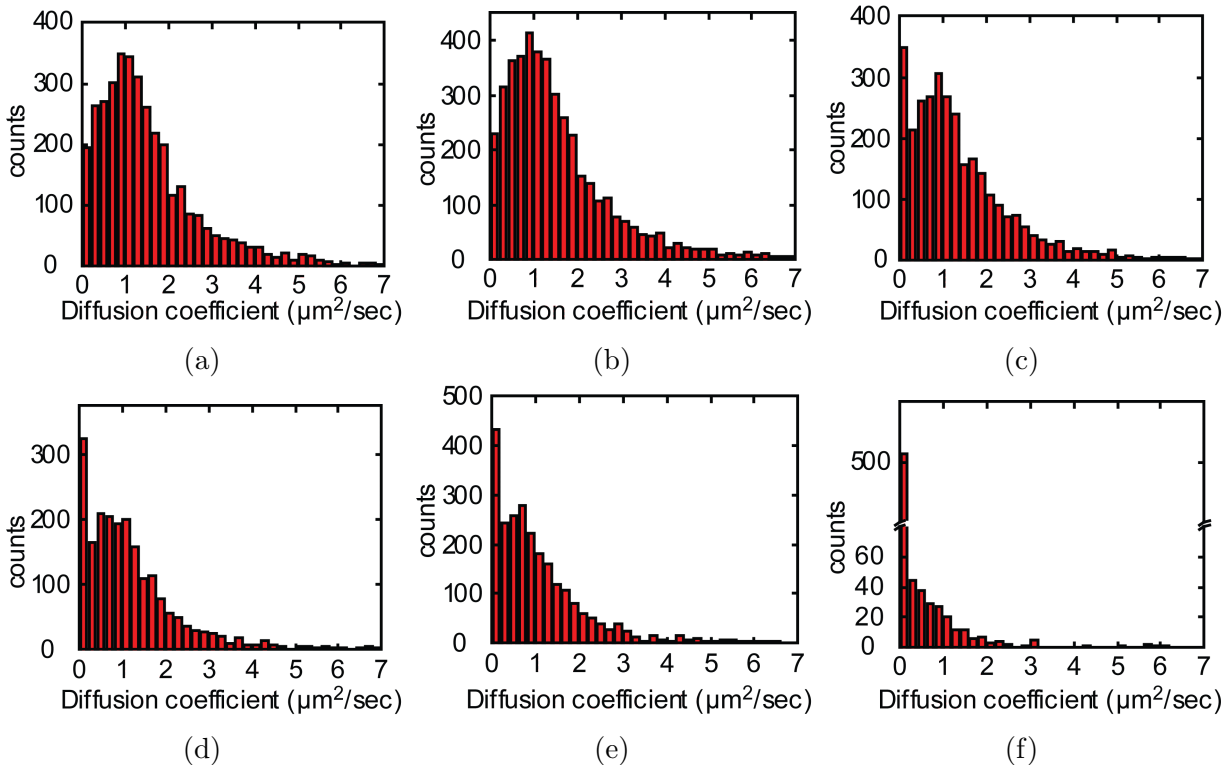


Figure 3.2: Distribution of diffusion coefficients. (a) 0% PEG w/v, (b) 10% PEG w/v, (c) 15% PEG w/v, (d) 20% PEG w/v, (e) 25% PEG w/v, (f) 37.5% PEG w/v. Figure (a) - (f) are distribution of the MSD slopes for C2 domains with increasing series of PEG concentration. Apparent diffusion coefficient can be calculated from MSD slope, $MSD/4\Delta = D$.

3.3.2 Effect of PEG on lipids

The membrane targeting C2 domains demonstrated both increasing and decreasing trends in their parameters with respect to increasing concentration of the crowding agent (PEG). Similar to chapter 2, in this experiment PC:PS are mixed in 3:1 ratio where PS is negatively charged and PC is neutral. Additionally we have 1% of fluorescent lipid (PE). After incubating fluorescent lipids bilayer for 30 minutes in the chamber well, we washed it extensively to flush away extra floating lipids. The fluorescent lipid bilayer is shown in figure 3.4. During this experiment, we fixed the aperture according to the size of ROI we needed to bleach. After bleaching, the fluorescent intensity of the molecules was minimized. Over time, the non bleached molecules diffused into the photo bleached area where it mixed with dark lipids. Recovery happened gradually with fluorescent molecules displacing the dark molecules. The primary goals of the experiment was to know the amount of time it took to recover the

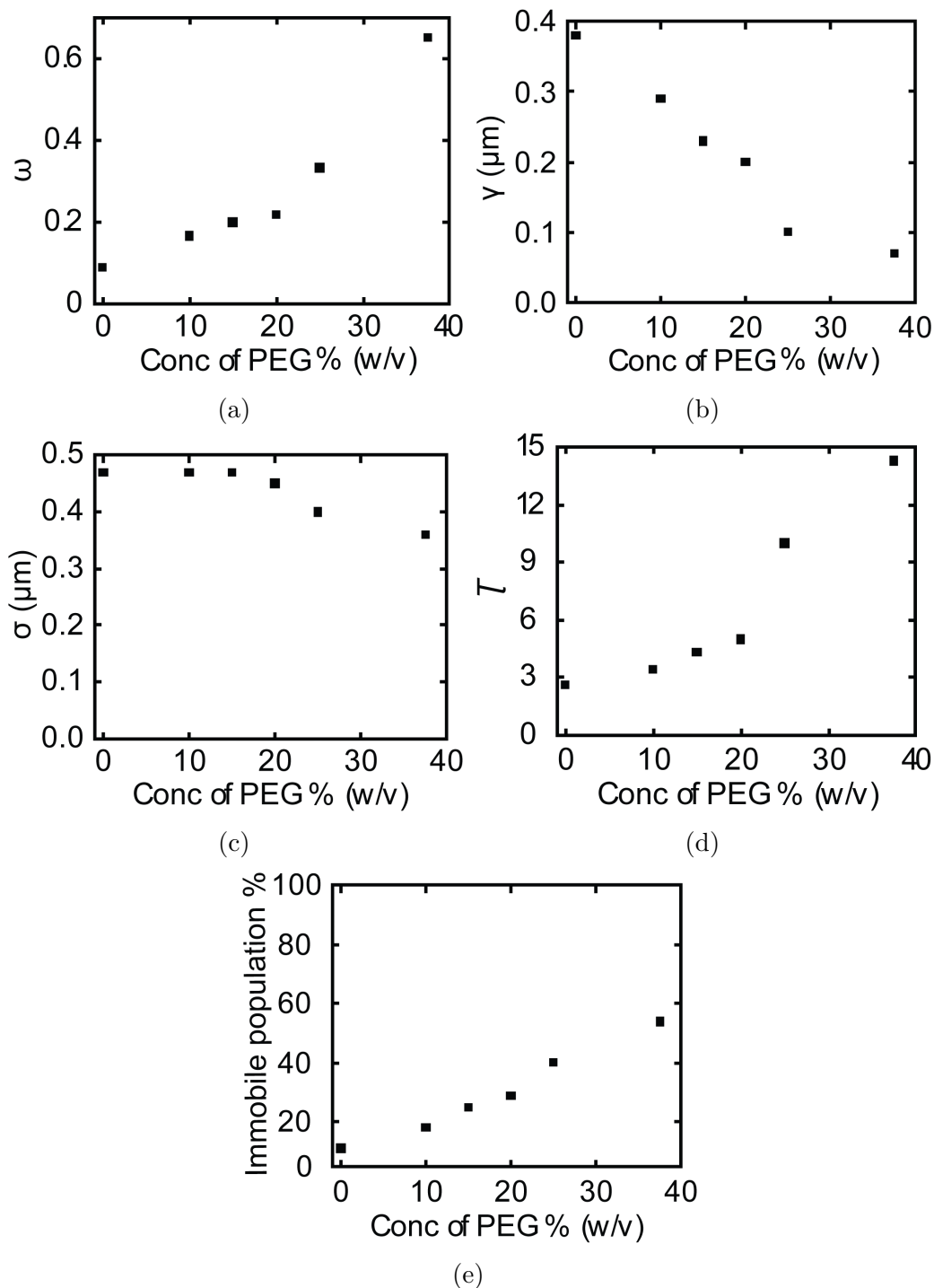


Figure 3.3: Effect of PEG on C2 domains. (a) ω is the fraction of molecules that jumped without including the immobile population. From figure (b), γ is the the transition between the surface and the bulk phase which corresponds to immobile molecules. From figure (c) σ gives the estimation of surface diffusion. From figure (d) τ_{des} is desorption time. From figure (e) immobile population is from the percentage of molecule population that does less than 280 nm displacement.

bleached area with fluorescent lipids and also to see if crowding agents affected this rate of diffusion by affecting the fluidity of the lipids. The results were obtained from fluorescent recovery after photobleaching (FRAP) technique. The pre-photo bleaching, photobleached, and recovering intensity as a function of time for each case is shown in figure 3.5 (a-f). Each recovery curve is fitted to a two phase exponential equation. The recovery of lipids for each PEG percentage ranged from 80-90%. The main take away from these results is that there is no trend in recovery from the diffusion of lipids as there was in case of membrane targeting C2 domains protein as shown in figure 3.5 and 3.6.

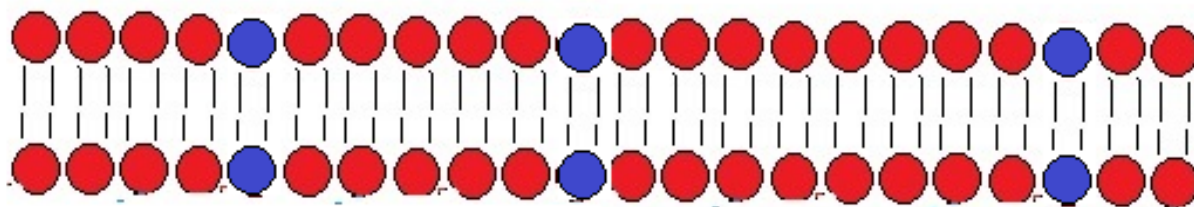


Figure 3.4: Fluorescent lipid on both sides of lipid bilayer

We saw in the results from figure 3.6 (a-b) that we had two recovery rate constants. The possibility for getting population of molecules with faster and slower rates which resulted in two phase exponential fit like in figure 3.5 (a-f) might be because the fluorescent molecules on the bottom layer of the bilayer are influenced by close proximity between them and cover glass surface. The lipids on bottom leaflet primarily diffused through the contact with glass which slowed down their diffusion. This does not commonly occur in vivo and it was probably artifact of our in vitro system. Other labs has conducted similar experiments where the supported lipid bilayer system was used. They also suggested to use double exponential fit because their data did not fit well to single exponential as well [62] [62]. After we fit to a double exponential and we found that fast rate contributed to most of the amplitude and a smaller amplitude had potentially less fluorescent molecules. However because of these two recovery rates, we fit our data to two phase exponential association as shown in equation 3.4 [63].

$$Y = Y_o + A_1[1 - e^{(-x/t_1)}] + A_2[1 - e^{(-x/t_2)}] \quad (3.4)$$

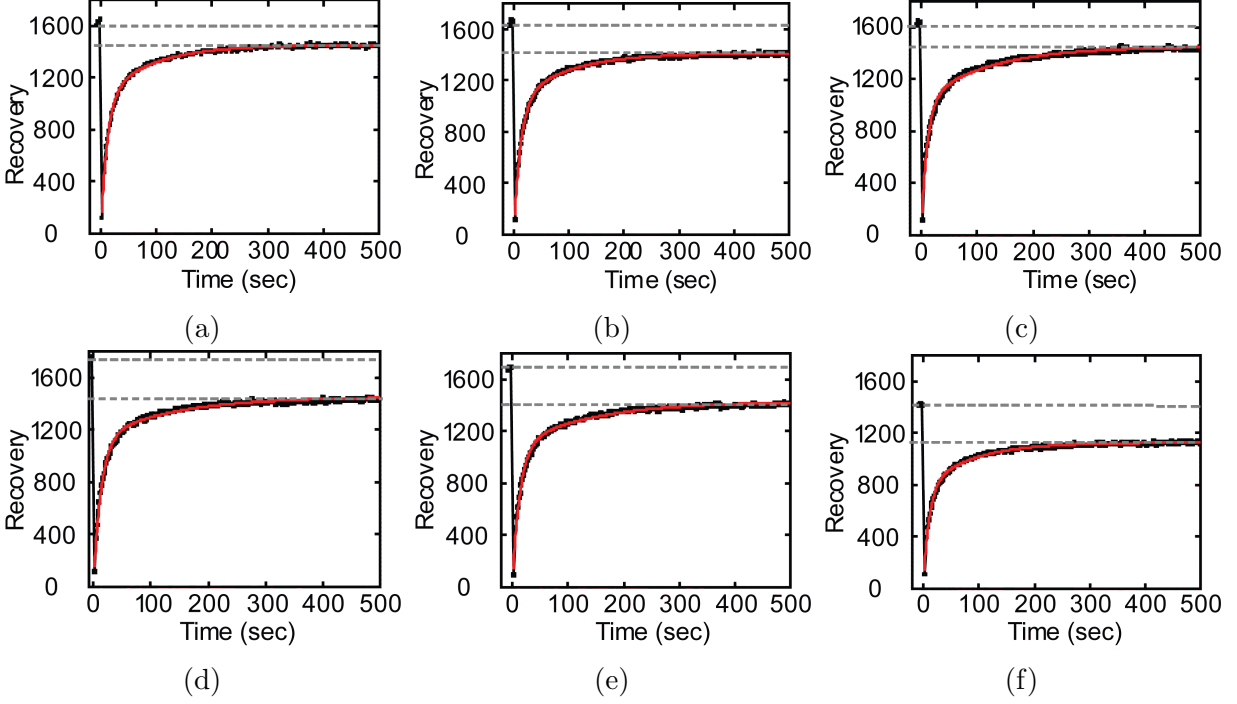


Figure 3.5: Intensity recovery in FRAP w.r.t series of PEG concentration. (a) 0% PEG w/v, (b) 10% PEG w/v, (c) 15% PEG w/v, (d) 20% PEG w/v, (e) 25% PEG w/v, (f) 37.5% PEG w/v. FRAP recovery curves of fluorescent lipids with 0%, 10%, 15%, 20%, 25%, 37.5% PEG respectively. Respective percentage of PEG w/v is added onto lipids to observe if the recovery times and diffusion rates changes (decreases). The incomplete recovery is because of some fraction of molecules that are immobilized on the bleached region of interest. These are immobile fractions. But the molecules that diffuses around and contributes to increase in intensity of that particular ROI are the mobile fraction. The area between the two dashed gray lines in figure 3.5a, 3.5b, 3.5c, 3.5d, 3.5e, 3.5f are the immobile fraction where as area from bottom dashed line to the origin line are the mobile fraction.

which can be simplified as $Y = Y_o + A_T[1 - \frac{A_1}{A_T}e^{(-x/t_1)} - \frac{A_2}{A_T}e^{(-x/t_2)}]$ where Y_o is the offset, A_1 is the maximum height of the first phase of curve from baseline, A_2 is the maximum height of the second phase of curve from baseline, t_1 and t_2 are the two recovery times in seconds. From the figure 3.6 (a-i), we did not see increasing or decreasing trend on the lipids diffusion. Another plot was the exponential curve 3.5 (a-f) with respect to time where we kept the pre-bleach intensity along with recovery points to show that how much recovery was achieved. We lost 15-20% of intensity. Error bars in all figures of 3.6 (a-i) are the standard error. Dashed gray lines were drawn on figure 3.5 (a-f) to mark the mobile points so that we noticed the difference between recovered and initial data. This showed percentage of molecules that

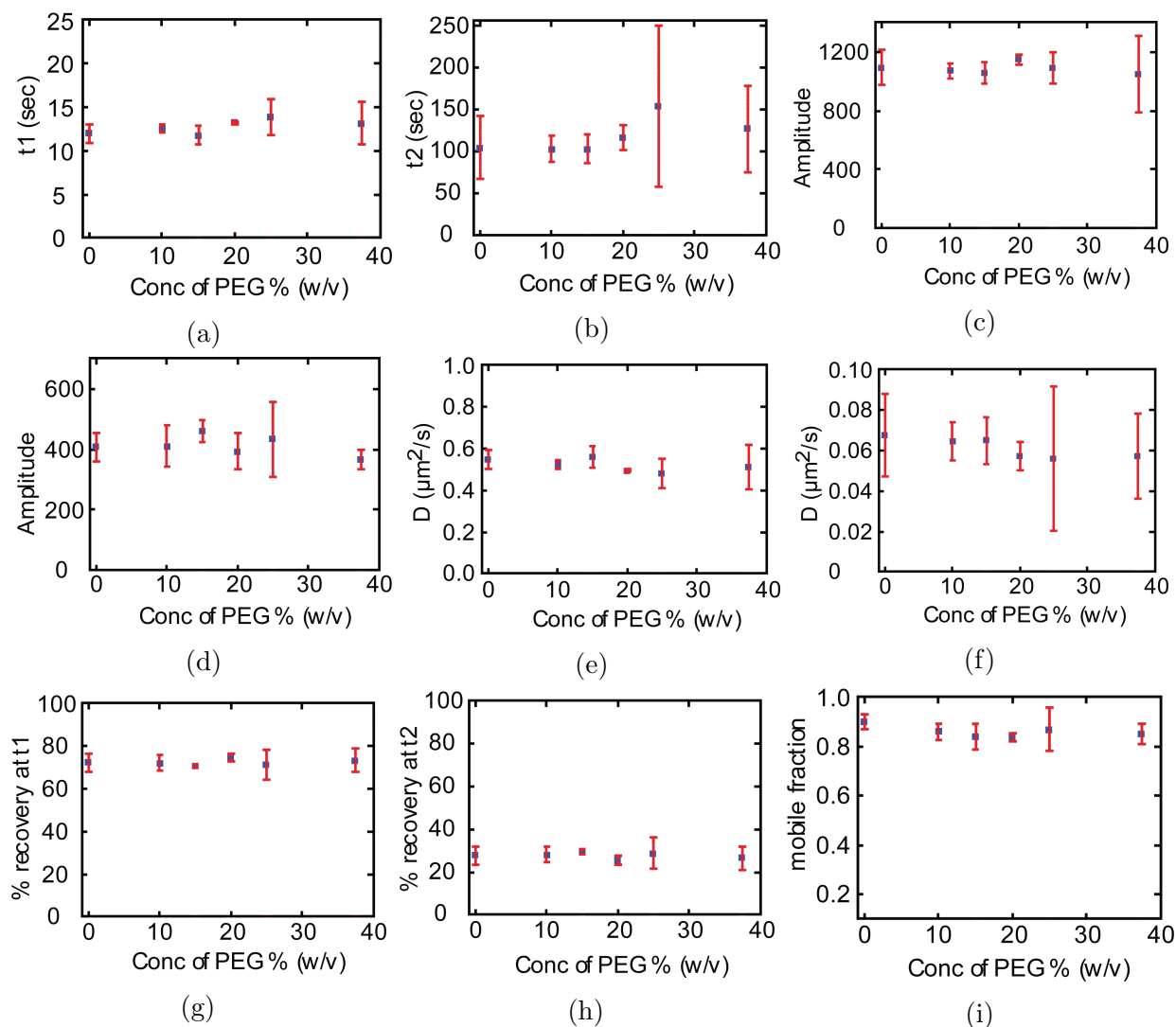


Figure 3.6: Results from FRAP experiment. (a) t_1 (rate 1) faster rate of recovery, (b) t_2 (rate 2) slower rate of recovery, (c) A_1 (Amplitude 1) Amplitude of faster recovering molecules, (d) A_2 (Amplitude 2) Amplitude of slower recovering molecules, (e) D_1 (Diffusion Coefficients 1) Diffusion coefficients of molecules recovering faster, (f) D_2 (Diffusion Coefficients 2) Diffusion coefficients of molecules recovering slower, (g) molecule percentage recovery at t_1 , (h) molecule percentage recovery at t_2 , (i) mobile fraction. Frap recovery times (t_1 and t_2), respective amplitude of each recovery times (A_1 and A_2), respective diffusion coefficients of each recovery times (D_1 and D_2), respective percentage recovery in each recovery times and mobile fraction when series of PEG concentration of fluorescent lipids with 0%, 10%, 15%, 20%, 25%, 37.5% PEG respectively. Respective percentage of PEG w/v is added onto lipids to observe if the recovery times and diffusion rates changes (decreases) Faster Rate of lipid recovery

diffused into the bleached spot. Cross profile was done in image J to verify the size of the bleached area which was $8.5 \mu\text{m}$. Figure 3.6 (a-b) shows percentage of molecules recovering at two recovery times. Two diffusion coefficients (D1 and D2) shown in figure 3.6(e-f) are from molecules recovering at two times (T1 and T2) which were calculated from equation 3.5.

$$D = \frac{\omega^2}{4t_{1/2}} \quad (3.5)$$

In equation 3.5, ω was the bleach radius and $t_{1/2}$ was the half recovery time [34]. Only purpose of reporting diffusion coefficient value here was to show that it did not form any trend with respect to increase in PEG concentration as shown in figure 3.6 (e-f). The difference in diffusion coefficients of lipids from literature was because our FRAP setup was not a perfect confocal FRAP and radius of bleached area was not automated but was a manual aperture. We aim to perform confocal FRAP in future experiment to verify the diffusion coefficients. In addition to FRAP technique we can use comparably efficient technique "single particle tracking" method to track low concentration of fluorescent lipids.

Another parameter we checked was mobile fraction which was calculated by equation 3.6.

$$\text{Mobile fraction} = \frac{I_{final}}{I_{beforephotobleaching}} \quad (3.6)$$

In equation 3.6, I_{final} was the intensity of the last final frame. $I_{beforephotobleaching}$ was the intensity of the frame before photo bleaching. There was no trend in mobile fraction when we did the titration of different percentage of PEG on lipids. The increasing recovery was the increase in amplitude. The higher the amplitude, the higher the content of fluorophore.

3.4 Conclusion

Our goal in chapter 2 was to see if kinetics of membrane targeting domains were affected by long jumps where motion of molecules deviated from simpler two dimensional diffusion. Our observations were explained in terms of bulk excursion that introduced jumps with heavy tail distribution. Results from chapter 3 continued to strongly show that superdiffu-

sion was caused by bulk-mediated diffusion where molecules dissociated from the membrane and performed three-dimensional random walks until they reached the membrane again and re-adsorbed at a new location. We described experimental results of superdiffusion of membrane-targeting C2 domains on supported lipid bilayers. It has been shown that the hunting process is extensively more efficient when relocation times are power-law distributed, resulting in a Lèvy walk [64]. The result of membrane hopping is that C2 domains remained in its near neighborhood for a short time and then hopped to a site that was far away than what could be covered by two-dimensional diffusion. This hopping hunt method was to discover bigger region so that C2 molecule could find a way around diffusion obstacle that might be present in the membrane. This jumping made the search process less exhaustive. In addition to these results, in chapter 3 we aimed to see if there was any effect in kinetics of the same membrane targeting C2 domains and their jumps in presence of crowding agent. Measurements of the distribution of displacements of membrane-targeting C2 domains in presence of crowding agent (PEG) were also performed by single-particle tracking. We observed the change in bulk excursions that introduced jumps with heavy tail distribution in presence of crowding agent. We saw many interesting effects like the strong trend in γ , τ_{des} , ω , σ with respect to percentage w/v increase of PEG. FRAP experiment was done to examine the source of the changes observed in diffusion of membrane targeting C2 domains proteins. We aimed to understand whether increasing concentrations of crowding agent (PEG) affected diffusion of proteins or diffusion of the lipids. The results in Fig 3.6a - 3.6i clearly showed that the fluidity of the lipids were not affected by the crowding agents which means that the interaction between the crowding agent and lipids had no considerable effect on diffusion of lipids. The recovery percentage of the mobile molecules and recovery times were measured by FRAP technique. The sample lipid was 3:1 ratio mixture of PC:PS with 1% fluorescent PE as function of series (0%, 10%,15%, 20%, 25%, 37.5%) w/v concentration of crowding agent(PEG). We obtained the double exponential fit for the recovery data. The faster component of t corresponded to the recovery time of the lipids on the upper leaflet and slower component of t corresponded to the diffusion from lipids in contact to cover glass surface. In our FRAP experiments, the bleached spot was circular, recovery occurred through the entire circumference of the spot lightening up the circular area. The

rate and amplitude of recovery was depending upon the contribution of kinetic fractions. A mobile lipids started to diffuse in before the first frame was collected after photo-bleaching. This rapid diffusion also had a mixture of slow diffusing molecule. The purpose of FRAP technique was to understand if proteins were hitting viscous drag of the crowding agent or if the lipid bilayers were becoming less fluid. After doing FRAP, we realized that the slowing effect was due to viscous drag experienced by membrane targeting C2 domains and not due to changes in fluidity of lipids.

TETHERED PARTICLE MOTION OF DNA AND RNA WITH RNA EXTENSION
EXPERIMENT³

4.1 Introduction

4.1.1 Purpose of experiment

The ultimate goal for this project was to observe real time polymerization of RNA by a polymerase, 3D pol, at a single molecule level on the supported lipid bilayer. The 3D pol is a RNA dependent RNA polymerase. The condition of this poliovirus RNA-dependent RNA polymerase plays a vital role in the genomic evolution of the virus [65]. There are various experimental approaches to understand this mechanism. We implemented two methods to understand the processes. One was tethered particle motion (TPM) and the other was flow extension of RNA. A bead is tethered to a DNA, and even in absence of any external force, this bead shows Brownian motion. TPM approach was first seen by Schafer et al in the early 1990's [66]. This method was used to understand the rate variation of a transcription process. In the TPM experiments, DNA/ RNA molecules were bound to the glass surface on one end while the other end was attached to a streptavidin bead. We incubated beads with DNA/ RNA so that they bound one end of a DNA/ RNA molecule and the other end stuck to the glass surface to immobilize it. Bright field video microscopy was used to observe the Brownian motion of the beads. The tracking and image analysis led us to understand the amplitude variation of the bead motion caused by DNA/RNA. We aimed to track each bead individually to determine the length of the DNA molecule tethered to a bead. The amplitude of the motion of a bead was determined from the standard deviation of the bead within a certain time interval. This led us to understand the distribution of bead positions known as the Boltzman distribution. Persistence and contour length was acquired from the

³For these set of experiments credits are : Grace Campagnola, Olve B. Peersen and Diego Krapf conceived the experiments. Olve B. Peersen and Diego Krapf supervised the project; Grace Campagnola, Bryce W. Schroder and Kanti Nepal conducted the experiments; Results presented here are analysed by Kanti Nepal.

total length of a DNA. The amount of bead movement depended upon the length of the DNA. The extent of deviation for a stiffer and more packed polymer was less than that of a flexible molecule. Using the same Boltzman distribution, we found the spring stiffness of a DNA. To understand the purpose of this experiment we needed to know the essential biology and mechanics of DNA/ RNA.

The proteins involved in polymerization has the capability to bend and twist the flexible DNA during repair and copy. DNA being a partially flexible polymer is modeled as a 'worm like chain' (WLC) model depending upon its bending firmness [67]. The WLC model explains the mechanics of partially flexible polymers and the structure of the DNA as a curve with a definite correlation length in the direction along the contour length [68]. Correlation length is a persistence length of the DNA. The flexibility and elasticity of the DNA comes from the persistence length. In the absence of any external force, DNA molecules could take a 3 dimensional (3D) shape [69]. The 3D shape is caused by bending mechanisms [67] like intercalation of hydrophobic amino acids between base pairs, a combination of phosphate attraction to each transiently-bound cation and repulsion of other solvent cations that would otherwise tend to screen phosphate charges [70]. It takes a lot of energy to bend a short DNA, whereas less energy to bend a longer DNA. This bending length is called persistence length. In our TPM experiments, we aimed to analyze the motion of a bead tethered to a glass slide by a single DNA. DNA molecules undergo Brownian motion in the absence of externally applied force. Thermal fluctuations and elasticity of DNA/ RNA affects the radius of the bead's Brownian motion [71]. Using a white light microscopy, the images of the constrained Brownian motion of beads attached to DNA at different positions were captured. A bead tethered to a DNA exhibited a confined Brownian motion. In one field of view, we manually selected beads performing the largest amplitudes of Brownian motion. We expected one bead to tether to one DNA molecule so that we could analyze single tethered DNA that did the circular symmetric Brownian motion in reference to an attached point.

4.2 Methods and materials

Detailed protocol is explained in the Appendix A.10- A.18.

4.2.1 Surface passivation

24 x 50 mm coverslips were cleaned with detergent water. After rinsing they were again dipped in 1M KOH, rinsed and dried with nitrogen gas. After plasma etching, the coverslips were APTES(Amine propyl triethyl silane) coated with acetone and were nitrogen dried. Then Aptes treated coverslips were baked. The first round of passivation was done with biotinylated NHS-ester PEG (Laysan Bio Inc., Catalog number 143-72). 70 μ l of this mixture was dropped onto one side of a coverslip and another coverslip was kept above it to make a sandwich. This sandwich was left to incubate overnight in a humid environment. The next day it dried and a second round of passivation was done. 70 μ l of mixture of DST, DMSO, and sodium bicarbonate was dropped on the coverslip to make a new sandwich, which was incubated for 2 hours. After rinse and dry these coverslips were ready to use.

4.2.2 Flow based chamber preparation

Glass/ plastic slides (PEARL microscope slides, catalog number: 7101) were drilled to make 6 holes, 3 on each of the short ends for the inlet and outlet of the flowcell. A rubber/metal (hand made) template was designed in a shape of the flow cell. The template was placed on double sided tape and the coverslips were attached to the other side of the tape to form a flow chamber. Then the flow cell was ready to use.

4.2.3 Working of sample transfer setup

The flow transfer setup was built in lab by former graduate student Bryce W. Schroder. The setup was organized in such a way that there were three knobs for three lines on the same flowcell. Each line had its own inlet and outlet. The tubes were connected together to make one single outlet to the waste container. Each knob had 5 available switch positions. Each switch position had its own inject and load function. When we injected the sample,

the knob was on the inject switch position, and when we loaded the sample, the knob was on the load switch position. When we needed to flow things to waste, the knob was on the waste switch position. While loading the sample, the sample first went to the loop tube. Then we turned on the syringe pump at a specific rate to push the sample from loop tube to one of the channels in the flowcell. Each flowcell was 15 μl and each loop was 250 μl . The tubes connected to the sample transfer setup were cleaned with MQ water each time before the experiment.

4.3 Results

4.3.1 Tethered particle motion of beads tethered to DNA and DNA stretching

We did experiments to record tethered particle motion where beads were tethered to DNA and performed Brownian motion. Among many beads found on one window of display, visually only few of them actually seemed to be doing TPM. This might be because of multiple tethers; although, DNA and bead ratio was targeted to be 1:1 to avoid multiple tethers. We determined standard deviation (SD) of motion as 140 nm which is root mean square end to end distance of double stranded 7 kb DNA.

$$\langle r^2 \rangle = \frac{Nb^2}{6} \quad (4.1)$$

In equation 4.1 $\langle r^2 \rangle$ is the root mean square end to end distance of 7kb DNA. In our calculations b is the Kuhn length, N is the number of segments.

$$L = \frac{7000}{3bp/nm} \quad (4.2)$$

$\approx 2.4 \mu\text{m}$ L is the contour length of the DNA.

$$b = \sqrt{L} \quad (4.3)$$

$\approx 50 \text{ nm}$ We also know that $b = 2A$ where A is persistence length.

$$N = \frac{L}{b} \quad (4.4)$$

$$= \frac{2400}{50} = 48$$

Back to

$$\langle r^2 \rangle = \frac{Nb^2}{6} \quad (4.5)$$

$$\sqrt{r^2} = \sqrt{\frac{N}{6}}b \quad (4.6)$$

which gives us: $= \sqrt{\frac{48}{6}} * 50 \text{ r} = 140 \text{ nm}$

To find the cutoff frequency at standard deviation of 140 nm, we needed to calculate spring constant of DNA because of entropy :

$$k = \frac{3k_bT}{2Ll_p} \quad (4.7)$$

In equation 4.7 k is the spring constant, L is the contour length, l_p is the persistent length.

Solving above equation, we get :

$$k = \frac{3 * 4.1 * 10^{-21}}{2 * 2400 * 10^{-9} * 25 * 10^{-9}} \text{ N/m}$$

$$k = 1.025 * 10^{-7} \text{ N/m}$$

We are trying to get τ where τ is the critical time to find cutoff frequency.

$$\tau = \frac{2k_bT}{KD} \quad (4.8)$$

In equation 4.8 K is the spring constant and D is the diffusion coefficient of 4um bead calculated from stokes equation.

$$D\zeta = K_B T \quad (4.9)$$

where $\zeta=6\pi\eta R$ Now, solving to find value of ζ .

$$=6 * 3.14 * \frac{4.5*10^{-6}}{2} \text{ kg/ms}$$

$$=8.90 * 10^{-4}\text{kg/ms}$$

$$=3.77 * 10^{-8}\text{kg/s}$$

$$\text{Now, } D=\frac{K_B T}{\zeta}$$

$$=\frac{4.1*10^{-21} \text{ Nm}}{3.77*10^{-8} \text{ kg/s}}$$

$$D= 0.1087\mu^2/\text{sec}$$

$$\text{Now, we substitute values to find: } \tau=\frac{2k_b T}{KD}$$

$$=\frac{8.2*10^{-21}*\pi}{1.025*10^{-7}*0.1087*10^{-6}}$$

$$=0.736 \mu\text{sec}$$

$$f_{cutoff} = \frac{3K_B T}{2\pi\zeta 2LL_p} \quad (4.10)$$

$$\text{soving for } f_{cutoff} : =\frac{4.1*10^{-21}}{1.897*10^{-20}} \text{ Hz}$$

$$=0.21 \text{ Hz}$$

Reciprocal of the standard deviation of this bead motion is the cutoff frequency. The cutoff frequency was found to be 0.21 Hz. DNA extension experiments were also performed by labeling DNA with sytox orange to visually observe the extension mechanism. We were able to see the length of extended DNA, and how the DNA changed as we changed the flow rate. The DNA used for this experiment was 13kb. Figures 4.1 (a-c) in this section are to show the effect of flow extension on DNA. No further analysis on these images were done.

4.3.2 RNA extension mechanism and experiment

RNA elongation experiment was conducted on transcript lengths of RNA transcribed for durations of: 20 seconds, 1 minute, 2 minutes, 3 minutes, 5 minutes and 15 minutes. These lengths were chosen to get a wide range of data for collecting ensemble measurements to show difference in each one of the transcription. We also took this approach so that we could find average stretching lengths of each RNA. 3D polymerase was used for transcription for this RNA for all of the above mentioned lengths. The RNA was ligated with biotin and dig on

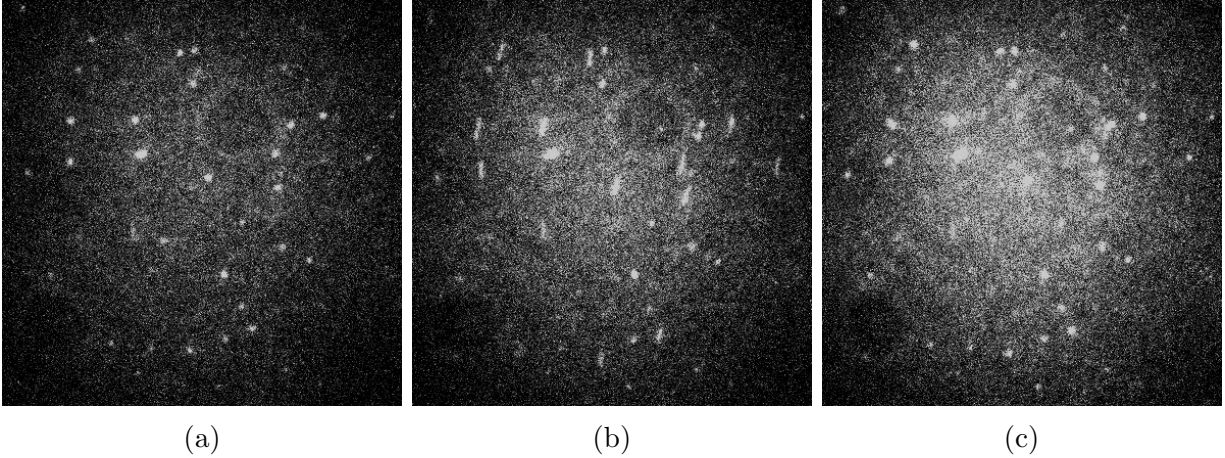


Figure 4.1: (a) DNA coiled up before stretching: Bright round spots are the DNA in absence of flow. (b) DNA stretching in response to flow: Bright elongated stretched spots are the DNA stretched in response to flow applied. (c) DNA stretching stops at this point when flow stops: Bright round spots of coiled DNA are seen again when flow is stopped.

either end with constant room temperature. These different sets of elongation times were achieved by quenching the transcription reaction using EDTA. The stretching process in the experiment was done by flowing buffer to the biotin tethered RNA and observing the bead's movement as flow continues [72]. The stretching mechanism of double stranded RNA and single stranded RNA was expected to be different as they have different mechanical properties [73]. Even the tethered particle motion behavior was expected to be different between double stranded and single stranded RNA. Before conducting this flow experiment, the RNA transcription was done by using 3D polymerase in a 15:1 ratio of polymerase to RNA with CTP and UTP to start the reaction, up to 20 nucleotides. In addition to textbook dsRNA and ssRNA, we observed that it was easier to work with dsRNA than ssRNA in our experiment.

Other experiments show that ssRNA formed complex structure that blocks the polymerase to perform transcription [72]. SsRNA was also more vulnerable to degradation than dsRNA [73]. Whereas, dsRNA had more stability, mobility, and reduced structure complexity [74]. In this flow based experiment, after RNA was tethered to the surface, flow of buffer was applied which stretched the RNA. This stretching was understood by the distance moved by the beads along the direction of the flow. This stretching showed the elasticity and

strength of that particular RNA. We observed the efficiency and speed of 3D polymerase to transcribe the ssRNA. The figure 4.2 showed clearly that the stretching increased as the flow rate increased. The figure 4.2 was from the 2-minute elongated RNA. Visually the stretching was seen, but further analysis was not done in doubt of sample swap. So, this figure 4.2 serves only as an example on how the stretching due to flow happens in real time.

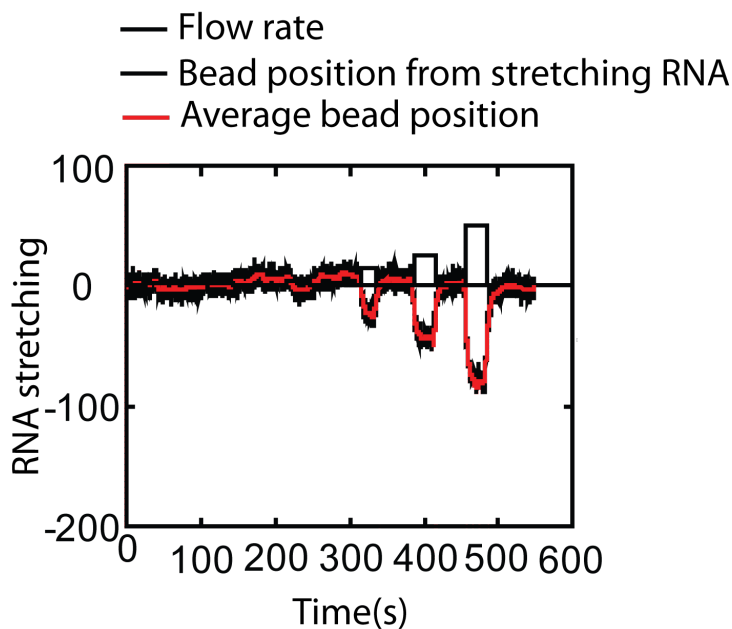


Figure 4.2: RNA stretching in response to increased flow rate: As flow rate increases RNA stretches respectively.

4.3.3 Amplitude measurement of tethered beads

In the TPM method, we aimed to track the individual trajectories/ positions of the beads in each frame. We used single particle tracking where the center of the bead was found and then we analyzed the bead position at nanometer precision scale. We used bright field imaging for this experiment. Each bead had its own distribution of successive bead positions. This analysis of diffusion of the beads within a given time gave us the magnitude of Brownian motion of DNA/ RNA tethered to the bead. We used the standard deviation of this distribution of each bead position to determine the Brownian motion. Depending on the length of dsDNA, the Brownian motion had to be linearly varying as the length of dsDNA increases. Mechanical drift or the distribution from more than one tethers was easily

distinguished from the single tethered DNA distribution. The distribution was expected to be round for single tethers where as distribution from multiple tethers was compromised and was found to be oval/elliptical [75]. This was possible because we analyzed beads with single molecule tracking techniques. However, experimentally, it was difficult to avoid the double tethers.

4.4 Discussion and conclusion

In this set of experiments, we used a RNA dependent RNA polymerase (3D polymerase) for polymerization of RNA from single strand to double strand. When attached to beads, we could observe each RNA polymerizing at the single molecule level by tracing the displacement of the beads. The tethered beads and RNA was provided with constant flow forces which stretched the strand and allowed polymerase to do its task to transcribe the second strand, depending upon the template strand. This method allows us to understand the rate and mechanism of polymerization. Once the task of polymerase was done, the difference in the structure between the initial single strand and later double strand could be observed through the tethered particle motion. When no force was applied the later double strand, RNA was expected to do a wider range of TPM than the initial single strand RNA. The elastic behavior of RNA was dependent on the rigidity of itself when it was being transcribed. The ultimate goal was to do the RNA transcription successfully on the synthetic lipid bilayer in-vitro. We observed the diffusion of proteins on the synthetic lipid bilayer which is described in chapter 2 and 3. One goal for future studies relevant to this project would be to understand the behavior of RNA dependent RNA polymerase to determine how their diffusion on lipid bilayer affects the whole transcribing mechanism. Single molecule imaging techniques should be used to analyze the transcribing mechanism of each RNA molecule.

CONCLUSION AND FUTURE WORKS

Chapter 1 describes the basic biology and introductory review of the research we choose for this thesis. Chapter 2 explains the non-ergodic, superdiffusive motion of membrane-targeting C2 domains in supported lipid bilayers. The motion was well described by Lèvy flights with jumps that had a heavy-tail distribution. The long jumps were caused by excursions into the liquid bulk. After dissociating from the membrane, the molecules diffused in three dimensions until they reached the membrane again and bound on a new location. Diffusion in the liquid bulk was much faster than diffusion in the membrane; therefore, we did not consider the delay time between dissociation and association. The surface distances covered by jumps had a Cauchy distribution, which was responsible for the heavy tail in the superdiffusive Lèvy flights. Model membranes provided an elegant system to study the effect of superdiffusive Lèvy flights because they were not subjected to interactions with other cell components that could mask its experimental observations. However, hopping was already observed on the surface of live cells [35] and we anticipate these processes to have broad physiological relevance in the surface diffusion of signaling molecules. Chapter 2 describes a future goal of this study to explore the effects of temperature and macromolecular crowding on bulk-mediated dynamics. Chapter 3 describes experiments that extends from chapter 2 to explain the effect of molecular crowding on the same membrane targeting C2 domains. We found convincing evidence showing that macromolecular crowding played a important role in cell biology and the proteins were affected as the concentration of the crowding agent increased. From our set of experiments, effects were seen in various forms like strong trends in γ , τ_{des} , ω , σ with respect to the percentage w/v increase of PEG. Literature showed many other effects like protein dynamics, oligomerization, aggregation, compartmentalization, folding etc. [76] [77]. Using PEG as a crowding agent helped us to mimic the in vivo crowded cell environment to some extent. One more goal of the study was to see the effect of temperature on the membrane targeting C2 domains, which was not done during my thesis period. We hope to understand that effect in the future. In addition to crowding agents (PEG) experiments, a

control experiment was performed to understand the effect of crowding agent on lipid bilayer. After seeing a dramatic trend in parameters affecting the membrane targeting C2 domains with an increase in PEG concentrations, we were concerned that this effect was coming from reduced lipid fluidity or was seen only on proteins. So, we did a FRAP experiment to identify this issue, which is also explained in subsection of chapter 3. The future goal identified in chapter 3 is to do a dual color imaging of the protein and lipid together. Dual color imaging can be done with an opto-split system by labeling lipids with one color and proteins with another. Such an analysis would provide more clear visualization of diffusion dynamics of proteins and lipids. Chapter 4 provides only preliminary and theoretical details because of experimental difficulties. We were not able to do experiments to measure the extension mechanism of RNA on the lipid bilayer and to observe real time polymerization of single strand RNA to double strand RNA.

Bibliography

- [1] V. Leiro, P. Moreno, B. Sarmiento, J. Durão, L. Gales, A. Pêgo, and C. Barrias, “Design and preparation of biomimetic and bioinspired materials,” *Bioinspired Materials for Medical Applications*, p. 1, 2016.
- [2] B. D. Ratner, A. S. Hoffman, F. J. Schoen, and J. E. Lemons, *Biomaterials science: an introduction to materials in medicine*. Academic press, 2004.
- [3] K. Dahl-Jørgensen, O. Brinchmann-Hansen, K. Hanssen, L. Sandvik, and O. Aagenaes, “Rapid tightening of blood glucose control leads to transient deterioration of retinopathy in insulin dependent diabetes mellitus: the Oslo study,” *Br Med J (Clin Res Ed)*, vol. 290, no. 6471, pp. 811–815, 1985.
- [4] J. Courtney, N. Lamba, S. Sundaram, and C. Forbes, “Biomaterials for blood-contacting applications,” *Biomaterials*, vol. 15, no. 10, pp. 737–744, 1994.
- [5] S. Martens, M. M. Kozlov, and H. T. McMahon, “How synaptotagmin promotes membrane fusion,” *Science*, vol. 316, no. 5828, pp. 1205–1208, 2007.
- [6] M. B. Jackson, “Inferring structures of kinetic intermediates in Ca^{2+} -triggered exocytosis,” *Curr. Top. Membr*, vol. 68, pp. 185–208, 2011.
- [7] A. Blicher, “Electrical aspects of lipid membranes,” Ph.D. dissertation, Ph. D. thesis, University of Copenhagen. http://www.nbi.ku.dk/english/research/phdtheses/phdtheses-2011/andreas-blicher/andreas_blicher.pdf. Accessed 1013 May 06, 2011.
- [8] B. Alberts, “The cell as a collection of protein machines: preparing the next generation of molecular biologists,” *Cell*, vol. 92, no. 3, pp. 291–294, 1998.
- [9] G. Isenberg and W. Goldmann, “Actin-binding proteins-lipid interactions,” *The Cytoskeleton: A Multi-Volume Treatise*, vol. 1, pp. 169–204, 1995.

- [10] C. Miller, J. Majewski, E. Watkins, D. Mulder, T. Gog, and T. Kuhl, “Probing the local order of single phospholipid membranes using grazing incidence x-ray diffraction,” *Physical review letters*, vol. 100, no. 5, p. 058103, 2008.
- [11] E. Watkins, C. Miller, D. Mulder, T. Kuhl, and J. Majewski, “Structure and orientational texture of self-organizing lipid bilayers,” *Physical review letters*, vol. 102, no. 23, p. 238101, 2009.
- [12] J. A. Dix and A. Verkman, “Crowding effects on diffusion in solutions and cells,” *Annu. Rev. Biophys.*, vol. 37, pp. 247–263, 2008.
- [13] H.-X. Zhou, G. Rivas, and A. P. Minton, “Macromolecular crowding and confinement: biochemical, biophysical, and potential physiological consequences,” *Annu. Rev. Biophys.*, vol. 37, pp. 375–397, 2008.
- [14] T. C. Laurent, “An early look at macromolecular crowding,” *Biophysical chemistry*, vol. 57, no. 1, pp. 7–14, 1995.
- [15] A. Weigel, “Characterizing the diffusional behavior and trafficking pathways of Kv2. 1 using single particle tracking in live cells,” Ph.D. dissertation, Colorado State University Libraries, 2007.
- [16] S. Denham and D. Cutchey, “Total internal reflection fluorescence (TIRF) microscopy: High contrast imaging of surface events.”
- [17] D. Axelrod, “Total internal reflection fluorescence microscopy in cell biology,” *Traffic*, vol. 2, no. 11, pp. 764–774, 2001.
- [18] N. Klonis, M. Rug, I. Harper, M. Wickham, A. Cowman, and L. Tilley, “Fluorescence photobleaching analysis for the study of cellular dynamics,” *European Biophysics Journal*, vol. 31, no. 1, pp. 36–51, 2002.
- [19] A. Chattopadhyay and M. Jafurulla, “Novel insights in membrane biology utilizing fluorescence recovery after photobleaching,” in *Biochemical Roles of Eukaryotic Cell Surface Macromolecules*. Springer, 2015, pp. 27–40.

- [20] G. Sitters, D. Kamsma, G. Thalhammer, M. Ritsch-Martel, E. J. Peterman, and G. J. Wuite, “Acoustic force spectroscopy,” *Nature methods*, vol. 12, no. 1, pp. 47–50, 2015.
- [21] K. M. Herbert, W. J. Greenleaf, and S. M. Block, “Single-molecule studies of RNA polymerase: motoring along,” *Annu. Rev. Biochem.*, vol. 77, pp. 149–176, 2008.
- [22] G. Yang, C. Cecconi, W. A. Baase, I. R. Vetter, W. A. Breyer, J. A. Haack, B. W. Matthews, F. W. Dahlquist, and C. Bustamante, “Solid-state synthesis and mechanical unfolding of polymers of T4 lysozyme,” *Proceedings of the National Academy of Sciences*, vol. 97, no. 1, pp. 139–144, 2000.
- [23] J. D. Watson and F. H. Crick, “Genetical implications of the structure of deoxyribonucleic acid,” *JAMA*, vol. 269, no. 15, pp. 1967–1969, 1993.
- [24] S. Brinkers, “All that glitters is gold: Nucleic acid detection using tethered gold,” Ph.D. dissertation, TU Delft, Delft University of Technology, 2011.
- [25] F. Crick *et al.*, “Central dogma of molecular biology,” *Nature*, vol. 227, no. 5258, pp. 561–563, 1970.
- [26] H. S. Bernhardt, “The RNA world hypothesis: the worst theory of the early evolution of life (except for all the others) a,” *Biology direct*, vol. 7, no. 1, p. 23, 2012.
- [27] G. Campagnola, K. Nepal, B. W. Schroder, O. B. Peersen, and D. Krapf, “Superdiffusive motion of membrane-targeting C2 domains.” *Scientific reports*, vol. 5, pp. 17 721–17 721, 2014.
- [28] W. Cho, “Membrane targeting by C1 and C2 domains,” *Journal of Biological Chemistry*, vol. 276, no. 35, pp. 32 407–32 410, 2001.
- [29] E. A. Nalefski and J. J. Falke, “The C2 domain calcium-binding motif: structural and functional diversity,” *Protein Science*, vol. 5, no. 12, pp. 2375–2390, 1996.
- [30] A. C. Newton, “Protein kinase C: structure, function, and regulation,” *Journal of Biological Chemistry*, vol. 270, no. 48, pp. 28 495–28 498, 1995.

- [31] I. Letunic, T. Doerks, and P. Bork, “SMART 7: recent updates to the protein domain annotation resource,” *Nucleic acids research*, vol. 40, no. D1, pp. D302–D305, 2012.
- [32] W. Cho and R. V. Stahelin, “Membrane binding and subcellular targeting of C2 domains,” *Biochimica et Biophysica Acta (BBA)-Molecular and Cell Biology of Lipids*, vol. 1761, no. 8, pp. 838–849, 2006.
- [33] J. H. Hurley, “Membrane binding domains,” *Biochimica et Biophysica Acta (BBA)-Molecular and Cell Biology of Lipids*, vol. 1761, no. 8, pp. 805–811, 2006.
- [34] J. D. Knight and J. J. Falke, “Single-molecule fluorescence studies of a PH domain: new insights into the membrane docking reaction,” *Biophysical journal*, vol. 96, no. 2, pp. 566–582, 2009.
- [35] M. Yasui, S. Matsuoka, and M. Ueda, “PTEN hopping on the cell membrane is regulated via a positively-charged C2 domain,” *PLoS Comput Biol*, vol. 10, no. 9, p. e1003817, 2014.
- [36] M. J. Skaug, J. Mabry, and D. K. Schwartz, “Intermittent molecular hopping at the solid-liquid interface,” *Physical review letters*, vol. 110, no. 25, p. 256101, 2013.
- [37] C. Yu, J. Guan, K. Chen, S. C. Bae, and S. Granick, “Single-molecule observation of long jumps in polymer adsorption,” *ACS nano*, vol. 7, no. 11, pp. 9735–9742, 2013.
- [38] J. A. Corbin, R. A. Dirkx, and J. J. Falke, “GRP1 pleckstrin homology domain: activation parameters and novel search mechanism for rare target lipid,” *Biochemistry*, vol. 43, no. 51, pp. 16 161–16 173, 2004.
- [39] A. V. Weigel, M. M. Tamkun, and D. Krapf, “Quantifying the dynamic interactions between a clathrin-coated pit and cargo molecules,” *Proceedings of the National Academy of Sciences*, vol. 110, no. 48, pp. E4591–E4600, 2013.
- [40] A. V. Weigel, B. Simon, M. M. Tamkun, and D. Krapf, “Ergodic and nonergodic processes coexist in the plasma membrane as observed by single-molecule tracking,” *Proceedings of the National Academy of Sciences*, vol. 108, no. 16, pp. 6438–6443, 2011.

- [41] K. Jaqaman, D. Loerke, M. Mettlen, H. Kuwata, S. Grinstein, S. L. Schmid, and G. Danuser, “Robust single-particle tracking in live-cell time-lapse sequences,” *Nature methods*, vol. 5, no. 8, pp. 695–702, 2008.
- [42] S. Sugita, O.-H. Shin, W. Han, Y. Lao, and T. C. Südhof, “Synaptotagmins form a hierarchy of exocytotic Ca²⁺ sensors with distinct Ca²⁺ affinities,” *The EMBO journal*, vol. 21, no. 3, pp. 270–280, 2002.
- [43] B. P. Ziemba and J. J. Falke, “Lateral diffusion of peripheral membrane proteins on supported lipid bilayers is controlled by the additive frictional drags of (1) bound lipids and (2) protein domains penetrating into the bilayer hydrocarbon core,” *Chemistry and physics of lipids*, vol. 172, pp. 67–77, 2013.
- [44] O. V. Bychuk and B. O’Shaughnessy, “Anomalous diffusion at liquid surfaces,” *Physical review letters*, vol. 74, no. 10, p. 1795, 1995.
- [45] J. D. Knight, M. G. Lerner, J. G. Marciano-Velázquez, R. W. Pastor, and J. J. Falke, “Single molecule diffusion of membrane-bound proteins: window into lipid contacts and bilayer dynamics,” *Biophysical journal*, vol. 99, no. 9, pp. 2879–2887, 2010.
- [46] R. Valiullin, R. Kimmich, and N. Fatkullin, “Lévy walks of strong adsorbates on surfaces: Computer simulation and spin-lattice relaxation,” *Physical Review E*, vol. 56, no. 4, p. 4371, 1997.
- [47] B. P. Ziemba, J. D. Knight, and J. J. Falke, “Assembly of membrane-bound protein complexes: detection and analysis by single molecule diffusion,” *Biochemistry*, vol. 51, no. 8, pp. 1638–1647, 2012.
- [48] Y.-H. M. Chan and S. G. Boxer, “Model membrane systems and their applications,” *Current opinion in chemical biology*, vol. 11, no. 6, pp. 581–587, 2007.
- [49] S. D. Hobson, E. S. Rosenblum, O. C. Richards, K. Richmond, K. Kirkegaard, and S. C. Schultz, “Oligomeric structures of poliovirus polymerase are important for function,” *The EMBO journal*, vol. 20, no. 5, pp. 1153–1163, 2001.

- [50] G. Margolin and E. Barkai, “Nonergodicity of a time series obeying lévy statistics,” *Journal of statistical physics*, vol. 122, no. 1, pp. 137–167, 2006.
- [51] J. E. Darnell, H. Lodish, D. Baltimore *et al.*, *Molecular cell biology*. Scientific American Books New York, 1990, vol. 2.
- [52] S. Singer and G. L. Nicolson, “The fluid mosaic model of the structure of cell membranes,” *Membranes and Viruses in Immunopathology; Day, SB, Good, RA, Eds*, pp. 7–47, 1972.
- [53] K. Honda, Y. Maeda, S. Sasakawa, H. Ohno, and E. Tsuchida, “The components contained in polyethylene glycol of commercial grade (PEG-6,000) as cell fusogen,” *Biochemical and biophysical research communications*, vol. 101, no. 1, pp. 165–171, 1981.
- [54] M. Jia, G.-Y. Sun, Y. X. Zhao, Z.-S. Liu, and H. A. Aisa, “Effect of polyethylene glycol as a molecular crowding agent on reducing template consumption for preparation of molecularly imprinted polymers,” *Analytical Methods*, vol. 8, no. 23, pp. 4554–4562, 2016.
- [55] R. I. Mahato, *Biomaterials for delivery and targeting of proteins and nucleic acids*. CRC Press, 2004.
- [56] S. Asakura and F. Oosawa, “Interaction between particles suspended in solutions of macromolecules,” *Journal of polymer science*, vol. 33, no. 126, pp. 183–192, 1958.
- [57] M. Weiss, H. Hashimoto, and T. Nilsson, “Anomalous protein diffusion in living cells as seen by fluorescence correlation spectroscopy,” *Biophysical journal*, vol. 84, no. 6, pp. 4043–4052, 2003.
- [58] J.-P. Bouchaud and A. Georges, “Anomalous diffusion in disordered media: statistical mechanisms, models and physical applications,” *Physics reports*, vol. 195, no. 4-5, pp. 127–293, 1990.
- [59] M. R. Horton, F. Höfling, J. O. Rädler, and T. Franosch, “Development of anomalous diffusion among crowding proteins,” *Soft Matter*, vol. 6, no. 12, pp. 2648–2656, 2010.

- [60] P. D. Ross and A. P. Minton, “Hard quasispherical model for the viscosity of hemoglobin solutions,” *Biochemical and biophysical research communications*, vol. 76, no. 4, pp. 971–976, 1977.
- [61] S. B. Zimmerman and A. P. Minton, “Macromolecular crowding: biochemical, biophysical, and physiological consequences,” *Annual review of biophysics and biomolecular structure*, vol. 22, no. 1, pp. 27–65, 1993.
- [62] K. J. Seu, L. R. Cambrea, R. M. Everly, and J. S. Hovis, “Influence of lipid chemistry on membrane fluidity: tail and headgroup interactions,” *Biophysical journal*, vol. 91, no. 10, pp. 3727–3735, 2006.
- [63] H. Kimura and P. R. Cook, “Kinetics of core histones in living human cells,” *The Journal of cell biology*, vol. 153, no. 7, pp. 1341–1354, 2001.
- [64] M. A. Lomholt, K. Tal, R. Metzler, and K. Joseph, “Lévy strategies in intermittent search processes are advantageous,” *Proceedings of the National Academy of Sciences*, vol. 105, no. 32, pp. 11 055–11 059, 2008.
- [65] X. Yang, E. D. Smidansky, K. R. Maksimchuk, D. Lum, J. L. Welch, J. J. Arnold, C. E. Cameron, and D. D. Boehr, “Motif D of viral RNA-dependent RNA polymerases determines efficiency and fidelity of nucleotide addition,” *Structure*, vol. 20, no. 9, pp. 1519–1527, 2012.
- [66] D. A. Schafer, J. Gelles, M. P. Sheetz, and R. Landick, “Transcription by single molecules of RNA polymerase observed by light microscopy,” *Nature*, vol. 352, no. 6334, p. 444, 1991.
- [67] J. S. Pedersen, “Analysis of small-angle scattering data from colloids and polymer solutions: modeling and least-squares fitting,” *Advances in colloid and interface science*, vol. 70, pp. 171–210, 1997.
- [68] C. Bouchiat, M. Wang, J.-F. Allemand, T. Strick, S. Block, and V. Croquette, “Estimating the persistence length of a worm-like chain molecule from force-extension measurements,” *Biophysical journal*, vol. 76, no. 1, pp. 409–413, 1999.

- [69] J. Samuel and S. Sinha, “Elasticity of semiflexible polymers,” *Physical Review E*, vol. 66, no. 5, p. 050801, 2002.
- [70] L. J. Maher, “Mechanisms of DNA bending,” *Current opinion in chemical biology*, vol. 2, no. 6, pp. 688–694, 1998.
- [71] C. Manzo and L. Finzi, “Chapter nine-quantitative analysis of DNA-looping kinetics from tethered particle motion experiments,” *Methods in enzymology*, vol. 475, pp. 199–220, 2010.
- [72] I. D. Vilfan, A. Candelli, S. Hage, A. P. Aalto, M. M. Poranen, D. H. Bamford, and N. H. Dekker, “Reinitiated viral RNA-dependent RNA polymerase resumes replication at a reduced rate,” *Nucleic acids research*, vol. 36, no. 22, pp. 7059–7067, 2008.
- [73] D. Dulin, I. D. Vilfan, B. A. Berghuis, S. Hage, D. H. Bamford, M. M. Poranen, M. Depken, and N. H. Dekker, “Elongation-competent pauses govern the fidelity of a viral RNA-dependent RNA polymerase,” *Cell reports*, vol. 10, no. 6, pp. 983–992, 2015.
- [74] J. Abels, F. Moreno-Herrero, T. Van der Heijden, C. Dekker, and N. Dekker, “Single-molecule measurements of the persistence length of double-stranded RNA,” *Biophysical journal*, vol. 88, no. 4, pp. 2737–2744, 2005.
- [75] P. C. Nelson, C. Zurla, D. Brogioli, J. F. Beausang, L. Finzi, and D. Dunlap, “Tethered particle motion as a diagnostic of DNA tether length,” *The Journal of Physical Chemistry B*, vol. 110, no. 34, pp. 17 260–17 267, 2006.
- [76] H.-X. Zhou, “Effect of mixed macromolecular crowding agents on protein folding,” *Proteins: structure, function, and bioinformatics*, vol. 72, no. 4, pp. 1109–1113, 2008.
- [77] S. R. McGuffee and A. H. Elcock, “Diffusion, crowding & protein stability in a dynamic molecular model of the bacterial cytoplasm,” *PLoS Comput Biol*, vol. 6, no. 3, p. e1000694, 2010.

Appendix A

MATERIALS LIST AND PROTOCOLS

Basically, this thesis is divided into two sets of experiments. The following are the two lists of materials, company/vendors for reagents and catalog number respectively used in each experiment.

A.1 Surface etching for lipid bilayer

Surface Etching is a necessary step for cleaning the coverslip before laying down lipids. Uncleaned surface will create background signals and disturb our analysis. Also our lipid bilayer might disrupt on uncleaned surface. The etching step helps to get rid of dirt and make the surface smooth too.

Materials, reagents and equipment

Materials:

- Coverslip holder (Diversified Biotech, Part number: WSDR 100)
- Water squirt bottle (Carolina biological, part number: 716613)
- 25 X 21 mm coverslips (Thermo Fisher, Richard-Allan Scientific , Catalog number: 102450)
- 20 ml beaker (Sigma Aldrich, part number: CLS100020 ALDRICH)

Reagents:

- Hydrogen Peroxide (Sigma Aldrich, catalog number 216763)
- Sulfuric acid: (EMD, catalog number: SX1244-5)

Equipment:

- Nitrogen gas source

Protocol

1. This protocol is used for TPM and RNA extension experiments.
2. Three coverslips are placed vertically (25 X 21mm) forming a triangle in 20 ml beaker. Depending upon number of coverslips we target to use, we can use more number of beakers.
3. 3:1 ratio of sulfuric acid to hydrogen peroxide is made to do piranha etching.
4. This mixture is poured into those 20 ml beakers and leave it for 45 minutes.
5. After 45 minutes, the coverslips are rinsed individually with water using squirt bottle.
6. Both sides are cleaned multiple times.
7. After rinsing all coverslips they are kept on the coverslip holder and again rinsed for 5-6 times. This should wash away the acid residue from the cover slip.
8. Rinsed coverslips are hold gently at the tip and nitrogen dried.
9. Once nitrogen dried, the slides are etched and is ready to use.

A.2 Cleaning Chamber wells

Chamber Wells cleaning is another necessary step before laying down lipids. Uncleaned chamber wells will not stick nicely to the coverslip which might cause leakage in between the experiment. This cleaning step helps to get rid of dirt from the chamber well and make them better sticking.

Materials, reagents and equipment

Materials:

- Chamber wells (Grace Bio-labs, catalog number 622105)
- Tweezers (Carolina biological, Item 624322)

- 25 X 21 mm coverslips: (Thermo Fisher, Richard-Allan Scientific , Catalog number: 102450)
- 50 ml conical tubes (Fisher scientific, Part number: 14-432-22)

Reagents:

- Ethanol: (Fisher Chemicals, catalog number: A962P-4)

Equipment:

- Nitrogen gas source
- Sonicating machine (Branson, catalog number: 1510)

Protocol

1. Chamber wells are placed into a 50 ml conical tube.
2. The plastic cover from chamber well is gently removed with help of tweezers.
3. 7 ml of ethanol and 33 ml of milli-Q is mixed to make 15% solution of ethanol. This can be anywhere between 10-20%. It helps chamber well to stick uniformly on coverslip.
4. The tube is sonicated for 10 minutes.
5. The chamber is rinsed 5-6 times with water.
6. The chambers and put in another dry conical tube after nitrogen drying.
7. Now, a unit of etched coverslip and chamber well can be made by sticking the chamber well at the center of coverslip.

A.3 Preparing the lipids - one day earlier and day of experiment

We need lipids to be free of chloroform before laying it down on the coverslip for experiment. Lipids when purchased comes in chloroform sealed package to stop them from forming a bilayer. But after arrival these lipids have to be dried down to get rid of chloroform.

Materials, reagents and equipment

Materials:

- Parafilm "M" (Bemis)
- 30 μ l glass tubes(Dabos, Product Code: 8372930)

Reagents:

- Lipids (Avanti polar lipids, catalog number: 244875)
- NaCl- Sodium chloride (Fisher Chemical, Catalog number: S271)

Equipment:

- Freezer
- Nitrogen gas source
- Sonicating machine (Branson, catalog number: 1510)
- Vaccum centrifuging machine (Dabos, Product Code: 7670562)

Protocol

1. This protocol is for lipid bilayer experiment.
2. The lipids come in a chloroform tight container while purchase.
3. The PC (phosphatidylcholine) and PS (phosphatidylserine) lipid containers are cracked open from neck.
4. The lipids are aliquoted into glass tubes.
5. The lipid tube are sealed tight with parafilm.
6. The lipids are nitrogen dried for 2-3 minutes until a thin film forms at the bottom of the tube.

7. After drying with nitrogen gas, glass tube is placed into a vacuum centrifuging machine overnight to get rid of the remaining chloroform and to dry the lipids even more.
8. Next day water is added into the dried lipids and the PC to PS are mixed as ratio required. For us ratio of PC: PS was 1:3.
9. The mixture was frozen for storage.
10. On the day of experiment, the frozen lipids are taken out from storage.
11. It is equilibrated into room temperature for a while.
12. It is wise to aliquot the lipid again into smaller volumes because the glass tubes might crack while sonication and all the lipids might be lost.
13. Lipids are sonicated until clear.
14. The lipids are mixed to NaCl in 1:1 ratio before laying it down on the etched coverslip. NaCl helps to swell the lipids and easily allows it to spread over the coverslip.

A.4 Preparing Buffer

This buffer is for lipid bilayer experiment. Various salts are mixed to make this buffer suitable for our experiment. Many steps of dilutions and mixing has to be done before starting experiment So we use this buffer throughout our experiment.

Reagents

Reagents:

- Calcium chloride (Fisher chemical, catalog number: 10035-04-8)
- DTT - Dithiothreitol (Thermo Fisher Scientific, catalog number: R0861)
- Hepes (Fisher Scientific, catalog number: 7365-45-9)
- Magnesium chloride (Fisher chemical, catalog number: 7791-18-6)
- NaCl- Sodium chloride (Fisher Chemical, Catalog number: S271)

Protocol

Target was to make 20 ml of buffer with following mixtures of salts:

1. 20 μ l of 1M Cacl (Fisher Scientific, catalog number: 10035-04-8)
2. 0.4 ml of 1M DTT (Thermo Fisher scientific,Catalog number: R0861)
3. 4 ml of 7.0 pH Hepes (Fisher Scientific, catalog number: 7365-45-9)
4. 80 μ l of 1M Mgcl₂ (Fisher chemical, catalog number: 7791-18-6)
5. Nacl- Sodium chloride (Fisher Chemical, Catalog number: S271)
6. 14.3 ml of water - MilliQ water (EMD Millipore, catalog number: Z00QSV0WW)

A.5 Preparing imaging setup

The lasers and microscope setup has to be switch on as well as aligned before we start the experiment. This process has to be done every time we do a new set of experiment. The samples are then brought to this imaging setup and video microscopy recording is done.

Equipment

Equipment:

- Camera
- Laser source
- Microscope
- Oil objective (Olympus 100X)
- Oil: (Olympus, catalog number: IMMOIL-F30CC)

Protocol

1. This imaging setup is for lipid bilayer experiment.
2. Power switch of the laser unit, computer unit, and camera is turned on.
3. The switch is pulled upward to bring microscope setup from STORM to TIRF.
4. Using the knob right next to TIRF switch, the angle of the laser is changed to bring it to the center.
5. Another knob right of that is used to change the beam size of laser.
6. After sample unit is placed on the microscope, TIRF angle has to set to get the perfect image.
7. The objective has to be 100X oil objective.
8. Stage has to be changed to the one that holds our 25 X 21 mm coverslip.
9. A drop of oil is dropped above the objective.

A.6 Conducting C2 domains and C2-GST control Experiment

Experiment conduction is the most vital step. After all the samples are ready, imaging setup is ready we continue to do the experiment. These experiments and recordings are done while our samples are mounted on the holder of microscope.

Materials, reagents and equipment

Materials:

- Chamber wells (Grace Bio-labs, catalog number 622105)
- Tweezers (Carolina biological, Item 624322)

Reagents:

- C2 protein - Original plasmid from Jeff Knight Denver.

- C2-GST dimer protein - Original plasmid from Jeff Knight Denver.
- Lipids (Avanti polar lipids, catalog number: 244875)

Equipment:

- Camera
- Laser source
- Microscope
- Oil objective (Olympus 100X)
- Oil: (Olympus, catalog number: IMMOIL-F30CC)

Protocol

1. 55 μ l of sonicated and clear lipids are incubated for 45 minutes into the coverslip-chamber well unit.
2. After 45 minutes, extra floating lipids are washed with 1ml of 1X concentrated Buffer.
3. A drop of oil is dropped on the back of coverslip unit.
4. After following all steps from "preparing imaging setup", the unit is placed on the microscope stage.
5. Few movies are taken of lipid bilayer alone before putting proteins. This works as the background for later to compare when proteins are put in.
6. Proteins are added onto the lipid bilayer from one hole of the chamber well and sucked out from another hole 4-5 times so that proteins spread well in the chamber unit.
7. The density of protein has to be good enough rather than following a fixed concentration. So, concentration of protein might vary in experiment.
8. Movies are taken as many as needed. 30 ms exposure was done.

9. These steps are repeated to image the lipid bilayer with new protein in new the chamber.
10. Instead of adding C2 protein, this time add C2-GST dimer was added as control experiment.
11. Movies were taken as many as needed.

A.7 Preparing PEG solution

Second goal of our experiment was to understand the effect from crowding agent. We chose PEG as our crowding agent. So, to conduct this series of experiment we made different percentage concentrations of PEG starting from 10, 15, 20, 25, 37.5.

Reagents

Reagents:

- PEG - Polyethylene glycol (Integra Chemical Company, catalog number: P560.31.30)
- NaCl- Sodium chloride (Fisher Chemical, Catalog number: S271)

Protocol

1. This protocol is for lipid bilayer experiment.
2. PEG is thick when made a concentrated solution. With experience it is learned that the highest percentage of PEG could be made is 37.5% w/v.
3. Dilution of PEG with water was done to make 50% w/v concentration. But the same buffer concentration is needed as lipids so that the crowding agent would not disrupt the bilayer.
4. 1 gm of PEG was weighed and diluted.
5. Then 1gm of PEG is mixed in 2 ml of water to make it 50% w/v dilute.

6. 37.5% w/v is the maximum concentration with buffer in the mixture.
7. Once 50% w/v PEG is made, $C_1 \times V_1 = C_2 \times V_2$ rule is used to make 10% w/v, 15% w/v, 17.5% w/v, 20% w/v, 22.5% w/v, 25% w/v, 37.5% w/v where C_1 is 50, V_1 is unknown term, C_2 is the percentage we want to make, V_2 is 1000 ml.
8. Now all separate tubes with variety of PEG percentages are ready to work.

A.8 Conducting experiment on C2 domains with crowding agent

After preparing series of PEG concentrations, we conducted experiment by adding these concentration of PEG one by one to our sample. Here our sample had non-fluorescent lipids and C2 domains proteins. As we were adding the PEG we were also recording the movies to analyze them later.

Materials, reagents and equipment

Materials:

- Chamber wells (Grace Bio-labs, catalog number 622105)
- Tweezers (Carolina biological, Item 624322)

Reagents:

- C2 protein - Original plasmid from Jeff Knight Denver.
- C2-GST dimer protein - Original plasmid from Jeff Knight Denver.
- Lipids (Avanti polar lipids, catalog number: 244875)
- PEG - Polyethylene glycol (Integra Chemical Company, catalog number: P560.31.30)

Equipment:

- Camera
- Laser source

- Microscope
- Oil objective (Olympus 100X)
- Oil: (Olympus, catalog number: IMMOIL-F30CC)

Protocol

1. The steps from 'Conducting C2 domains and C2-GST control Experiment' is repeated till adding C2 domains proteins on the lipid bilayer.
2. Movies are taken as needed.
3. Different percentages of PEG are added sequentially and movies are taken as needed for each one.
4. It is seen that diffusion of proteins slows down as the PEG concentration increases.

A.9 Conducting FRAP experiment

FRAP experiment is conducted to understand if there is any effect of crowding agent on the lipids too. We have seen that PEG effects the diffusion of proteins but this experiment was conducted to understand if PEG effects the fluidity of lipids or not.

Materials, reagents and equipment

Materials:

- Chamber wells (Grace Bio-labs, catalog number 622105)
- Tweezers (Carolina biological, Item 624322)
- 25 X 21 mm coverslips (Thermo Fisher, Richard-Allan Scientific , Catalog number: 102450)

Reagents:

- Lipids (Avanti polar lipids, catalog number: 244875)
- PEG - Polyethylene glycol (Integra Chemical Company, catalog number: P560.31.30)
- NaCl- Sodium chloride (Fisher Chemical, Catalog number: S271)

Equipments:

- Camera
- Laser source
- Microscope
- Oil objective (Olympus 100X)
- Oil: (Olympus, catalog number: IMMOIL-F30CC)
- Sonicating machine (Branson, catalog number: 1510)

Protocol

1. This protocol is is lipid bilayer experiment.
2. The 55 μ l of sonicated fluorescent lipids are incubated into the coverslip - chamber well unit for 45 minutes.
3. After 45 minutes, the extra floating lipids are washed with 1 ml of 1X concentrated Buffer.
4. A drop of oil is dropped on the back of coverslip unit.
5. After following all steps from " preparing imaging setup", the unit is placed on the microscope stage.
6. Movies are taken as needed.
7. Different percentages of PEG are added sequentially and movies are taken as needed for each one.
8. It is seen that diffusion of lipids are not affected as the PEG concentration increases.

A.10 Surface passivation for TPM and RNA extension experiment

Surface passivation is the step where we coat our coverslip with layers of chemicals listed below. These coating are done so that the binding between our samples and surface is made in the mean time we should be able to eliminate any non specific bindings.

Materials, reagents and equipment

Materials:

- Aluminium foil (Reynolds wrap)
- Coverslip holder (Diversified Biotech, Part number: WSDR 100)
- Dish detergent (Planet scent free)
- Hazardous waste container (Any finished bottle)
- Parafilm "M" (BEMIS)
- Sealing ziplock bag (Ziplock vaccum)
- Tweezers (Carolina biological, Item 624322)
- 24 X 50 mm coverslips (Thermo Fisher, Richard-Allan Scientific , Catalog number: 152450)
- 100 ml beaker (Sigma Aldrich, part number: CLS1000250 ALDRICH)

Reagents:

- IPA - Isopropanol (EMD Millipore Corporation, Catalog number 67-63-0)
- 1 M KOH (Fisher Scientific, catalog number: P258-212)

Equipment:

- Air objective (Olympus 40X)
- Camera

- Microscope
- Nitrogen gas source
- Sonicating machine (Branson, catalog number: 1510)

Protocol

1. Required number of 24 x 50 mm coverslips are placed in coverslip holder.
2. The holder is kept in 100 ml beaker
3. The beaker is filled with distilled water and a generous amount of dish detergent is added.
4. Water level of sonicator has to be checked if it is good and place the beaker with coverslips in it.
5. To remove dust, dirt, oil from surface of coverslip, sonication is done for 20-30 minutes.
6. The coverslips are rinsed multiple times with milli-Q water to remove all soap residue.
7. After soap bubbles are no longer seen, the beaker is refilled with water transport back to sonication area.
8. The beaker is emptied and refilled with 1 M KOH just till above the top of the holder.
9. Coverslips are now sonicated for atleast 20 minutes in 1 M KOH.
10. Beaker is covered with parafilm or aluminium foil.
11. After sonicating KOH is poured into hazardous waste container with proper label and date.
12. Coverslip are rinsed 3 times with milli-Q water and transport to area of nitrogen gas.
13. Coverslips are holded one by one with help of tweezers.
14. Tweezers are cleaned with IPA and dried it before using.

15. Once the surface is completely dried, it is placed on the clean container for further use.
16. If intended to use the cover slip for future use, the moisture sealing silicon bag has to be kept in the container. Also tight seal has to be done using parafilm. This type of stored coverslips are good to use for a year or so.

A.11 APTES (Amine propyl trithyl silane) coating

This is yet another process of surface coating. This step also serves same purpose like that of surface passivation.

Materials, reagents and equipment

Materials:

- Aluminium foil (Reynolds wrap)
- Coverslip holder (Diversified Biotech, Part number: WSDR 100)
- Hazardous waste container (Any finished bottle)
- Parafilm: BEMIS Flexible Packaging.
- Tweezers (Carolina biological, Item 624322)
- 1000 ml beaker (Sigma Aldrich, catalog number: CLS100050 ALDRICH)
- 24 X 50 mm coverslips (Thermo Fisher, Richard-Allan Scientific , Catalog number: 152450)

Reagents:

- APTES - Amine propyl trithyl silane (Sigma Aldrich, catalog number: 440140 ALDRICH)
- IPA - Isopropanol (EMD Millipore Corporation, Catalog number 67-63-0)
- 1M KOH (Fisher Scientific, catalog number: P258-212)

- 400 ml acetone (Sigma Aldrich catalog number: 179973 SIGMA-ALDRICH)

Equipment:

- Biosafety Fume hood
- Baking oven
- Nitrogen gas source
- Plasma etching machine (Plasma Etch, catalog number: PE-50 Venus)

Protocol

1. This protocol is for TPM and RNA extension experiment.
2. The KOH treated coverslips are plasma etched.
3. While plasma is running, APTES solution is prepared in 1000 ml beaker.
4. 10 ml of APTES is poured in 400 ml of acetone in a beaker.
5. The mixture has to be swirled.
6. The mixture is covered with parafilm and transported back to plasma oxygenating area.
7. As soon as plasma oxygenating is completed, the coverslip is dip in APTES solution and cover with parafilm.
8. The APTES containing beaker with coverslip is sonicated for 20-30 minutes with 2-3 minutes interval to ensure good APTES coverage.
9. After sonication APTES solution has to be carefully poured into hazardous waste container with proper label and date in the fume hood.
10. Coverslips are rinsed with water multiple times and nitrogen dried the coverslip one by one.

11. Dried coverslips are kept in a dry holder and the dry holder into a dry beaker.
12. The beaker is covered with aluminium foil.
13. Aluminium foil has to be cleaned with acetone and IPA. Then nitrogen dried.
14. This beaker is placed into the oven at 100° for at least an hour fully dry and get uniform coverage.
15. While coverslips are baking, the first round of passivation can be started.

A.12 1st round of passivation

This step is first round of passivation. After this step our surface will be good to go for storage but has to be 2nd round passivated before use.

Materials, reagents and equipment

Materials:

- Coverslip holder (Diversified Biotech, Part number: WSDR 100)
- Old pipette tip box
- Parafilm "M" (BEMIS)
- Tweezers (Carolina biological, Item 624322)
- 1000 ml beaker (Sigma Aldrich, catalog number: CLS100050 ALDRICH)
- 24 X 50 mm coverslips (Thermo Fisher, Richard-Allan Scientific , Catalog number: 152450)

Reagents:

- Biotinylated NHS-ester PEG (Laysan Bio, Inc., Catalog number 136-156)
- IPA - Isopropanol (EMD Millipore Corporation, Catalog number 67-63-0)

- NHS-ester PEG (Laysan Bio Inc., Catalog number 143-72)
- 0.1 M sodium bicarbonate (Fisher Scientific, catalog number: MFCD00003528)

Equipment:

- Biosafety Fume hood
- Nitrogen gas source
- Vortexing machine (VWR, model number: Sw 945306)

Protocol

1. This protocol is for TPM and RNA extension experiments.
2. Biotinylated NHS-ester PEG and NHS-ester PEG are taken out from freezer.
3. It is allowed to equilibrate to room temperature.
4. 0.1 mg of Biotinylated NHS-ester PEG is needed per coverslip pair which means 40 coverslip means 20 coverslip pair.
5. 0.1 mg per 20 coverslips pair means 2.0 mg of biotinylated NHS-ester PEG is needed.
6. 8mg of NHS-ester PEG for a pair of coverslip is needed which means 160mg of NHS-ester PEG for 20 coverslip pair is needed.
7. Getting back to previous step, the exact amount of biotinylated NHS-ester PEG and NHS-ester PEG has to be weighed out with sensitive weighing scale.
8. The amount of time the powder remains in the air has to be minimized because moisture degrades these powder.
9. While coverslips are still baking, a humid chamber has to be setup for cover slip incubation. Old pipette tip box can be used because there will be a water reservoir in it.
10. Once slides are done baking they have to be taken to the hood to cool down.

11. While slides baking or cooling, the powder with 0.1 M sodium bicarbonate has to be diluted and vortex to dissolve.
12. 0.1 M Sodium bicarbonate solution needed. So 84 mg is dissolved in 10 ml water.
13. 64 μl per coverslip pair is needed so 1280 μl 0.1 M sodium Bicarbonate that is 1.28 ml is prepared.
14. 70ul of this mixture is dropped onto one side of one coverslip.
15. Another coverslip is put on top of the first one and make a sandwich.
16. In same manner 20 sandwiches are made. They are placed in multiple pipette box.
17. It is left to incubate over night in dark.
18. After over night incubation, coverslips are rinsed multiple times with water. The orientation has to be noticed when separating the sandwich.
19. After drying the coverslip, some marking has to be done on non-incubated side so that it will be easy to identify later.
20. Each dried cover slip is stored in single 50 ml conicals.
21. Those conicals are put in vacuum sealing ziplock bags. It has to be locked properly and vacuum sealed.
22. These slides are good to use for 6 months.
23. Although while using later, one must do second round of passivation too.

A.13 2nd round of passivation

This step is second round of passivation. After this step our surface will be ready to use or storage for future use.

Materials, reagents and equipment

Materials:

- Coverslip holder (Diversified Biotech, Part number: WSDR 100)
- Old pipette tip box
- Parafilm "M" (BEMIS)
- Tweezers (Carolina biological, Item 624322)
- 24 X 50 mm coverslips (Thermo Fisher, Richard-Allan Scientific , Catalog number: 152450)

Reagents:

- DST - disuccinimidyl tartrate (Thermo Scientific, Catalog number: 20589)
- DMSO - Dimethyl sulfoxide (Sigma- Aldrich, Catlog number: 472301)
- IPA - Isopropanol (EMD Millipore Corporation, Catalog number 67-63-0)
- 0.1 M sodium bicarbonate (Fisher Scientific, catalog number: MFCD00003528)

Equipment:

- Biosafety Fume hood
- Nitrogen gas source
- Refrigerator

Protocol

1. This protocol is for TPM and RNA extension experiments.
2. DST has to be crosslinked.
3. DST are taken out from refrigerator and allowed to equilibrate to room temperature.
This is done to minimize condensation on the vial as powder is moisture sensitive.

4. 0.68 mg DST is needed per coverslip pair. For example 10 coverslips is 5 pair.
5. As according to 0.68 mg per pair it needs to be 3.4 mg DST.
6. 4 μl of DMSO(Dimethyl sulfoxide) is dissolved per coverslip pair. 20 μl DMSO is needed.
7. 66 μl of 0.1 M sodium bicarbonate is added per pair.330 μl is needed.
8. 70 μl of this mixture is added to first round passivated coverslips on the previously coated side and incubated as sandwich again.
9. Incubation is done for 2 hours at room temperature in dark.
10. Rinsed and dried.
11. Now after this second round of passivation, the coverslips are ready to use.

A.14 Making a flowcell

This protocol is for TPM and RNA extension experiments. These flow cells are used to incubate the samples as well as conduct the flow stretching experiment. Flowcells are connected to tubes for delivering the samples and well as for outlet. Three channels are made with individual tubes.

Materials, reagents and equipment

Materials:

- Coverslip holder (Diversified Biotech, Part number: WSDR 100)
- Drilled glss/ plastic slides (PEARL microscope slides, catalog number: 7101)
- Double sided tape 3M Xseries (Fisher chemical, Catalog number: M- 12689)
- Knife
- Rubber/metal 3 channel template (hand made)

- 24 X 50 mm coverslips (Thermo Fisher, Richard-Allan Scientific , Catalog number: 152450)

Equipment:

- Biosafety Fume hood

Protocol

1. Glass/ plastic slides are drilled to make 6 holes, 3 on each short ends for the inlet and outlet of sample.
2. A template is made with rubber in a shape of the flow cell designed.
3. The template is placed on the double sided tape and cut it with little extra on sides with knife and tweezers.
4. The layer of tape found and cut it through to make shape of template on the double sided tape.
5. At the end of the double sided tape poke and pull out the cut portion.
6. Double sided tape is placed on the glass/ plastic slide without blocking the holes. Easier way to do it is by putting the double sided tape upside down on the slab and then placing the slide above it.
7. The excess double sided tape on sides are cut.
8. Double sided tape nicely spread over the slide so that it glues properly.
9. The back paper of double sided tape is pulled off from the glass slide.
10. Now this surface is sticky to stick the cleaned/etched/passivated coverslip.
11. Coverslip with non coated side up and coated side down are kept on sticky surface of glass slide.

12. One should try to center it as much as possible so that it covers all 6 holes for three inlet and outlet channels.
13. It has to be pressed gently so that it glues nicely but does not break off.
14. Now the flow cell is ready to use.

A.15 Conduct Tethered Particle motion (TPM) experiment

Tethered Particle motion experiments are conducted on the flowcell mounted on the microscope. The tethered beads are observed to record its displacements. Following protocol explains how to conduct this experiment.

Materials, reagents and equipment

Materials:

- Coverslip holder (Diversified Biotech, Part number: WSDR 100)
- Drilled glass/ plastic slides (PEARL microscope slides, catalog number: 7101)
- Parafilm "M" (BEMIS)
- RNAsesZAP (Sigma, catalog number: R2020)
- Tweezers (Carolina biological, Item 624322)
- 24 X 50 mm coverslips (Thermo Fisher, Richard-Allan Scientific , Catalog number: 152450)

Reagents:

- Anti digoxin beads (Spherotech Inc., catalog number: TP-20-2)
- Biotinylated beads(Spherotech Inc., catalog number: TP-08-10)
- DNA: (Integrated DNA technologies)

- IPA - Isopropanol (EMD Millipore Corporation, Catalog number 67-63-0)
- Neutravidin (Thermo Fisher Scientific, catalog number: 31000)
- RNA (Integrated DNA technologies)
- 0.1 M NaOH (Fisher Chemical, catalog number: M-12689)

Equipment:

- Air objective (ZEISS A-Plan 40X)
- Syringe pump (New Era Pump System)

Protocol

1. Home built sample transfer setup was used.
2. Lines cleaning has to be done with old flowcell.
3. Air has to be sucked out of lines as much as possible.
4. Many series of cleaning procedures has to be done to get rid of RNAses and other dirt.
5. RNAses free water is used to clean the lines, then 0.1 M NaOH, 1 nM EDTA has to be flowed in.
6. The new coverslip - glass/plastic slide sandwich has to be installed in a flowcell holder.
7. Lines has to be connected with each corresponding holes.
8. After cleaning, the series of incubation has to begin on new flowcell using a syringe pump to transfer samples.
9. Syringe pump could be programmed to run or it could be used manually on the pump itself with buttons on it.
10. Infusion rate has to be low such as 50 $\mu\text{l}/\text{min}$ when supplied to lines so that there is no rupture anywhere. But it could be as high as 250 μl while flowing to waste.

11. Knobs are there to choose the lines for flowing samples.
12. Air bubbles has to be ssucked our carefully at every steps.
13. Neutravidin solution (250 μ l) has to be flowed to a line. The volume capacity of a line in a flowcell is actually 15 μ l but the volume it takes for a sample to reach the flowcell and fill it is 250 μ l from the port.
14. Neutravidin has to be incubated for 10 minutes.
15. Next is to flow in biotinylated beads(250 μ l). These beads can be seen flowing in and binding to neutravidin bound surface with the camera software.
16. This biotinylated beads is used for fiducial marker so having 3-4 beads a window is enough to fulfill our purpose.
17. Next is to flow in RNA. It has to be incubated for 10-15 minutes so that it binds to neutravidin firmly.
18. Then antidig beads has to be flowed in so that this beads goes and binds to the free end of RNA.
19. After 10-15 minutes, buffer is flowed in to clean excess/ unattached antidig beads. Flow rate is low like 20 μ l/minutes so that there is no shearing off the tethered RNA.
20. Antidig beads are lot larger than biotin beads.
21. Now is the time to record a movie. The TPM motion is clearly seen on nicely tethered beads.

A.16 AFS chip surface passivation

AFS chip has one channel in it for the sample flow. It is also a flowcell. This chip also has to be passivated like we passivated the coverslip before. The samples has to tether to the AFS glass surface for our TPM or extension experiments.

Materials, reagents and equipment

Materials:

- AFS chip flowcell (Lumicks)
- Bleach (Any commercial bleach like Clorox)

Reagents:

- Anti digoxin beads (Spherotech Inc., catalog number: TP-20-2)
- BSA - Bovine serum albumin (EMD OmniPur, catalog number: 2910)
- Casein (Sigma, catalog number: C6780)
- DNA (Integrated DNA technologies)
- IPA - Isopropanol (EMD Millipore Corporation, Catalog number 67-63-0)
- PBS - Phosphate Buffered Saline (Sigma Aldrich, product number: A9226)
- Pluronic(Sigma, catalog number: P2443)
- 1mM sodium thiosulfate (Fisher Scientific., catalog number: 10102-17-7)
- 4.5 μm polystyrene beads (Spherotech, Catalog number: AP-05-100)

Equipment:

- AFS instrument (Lumicks)
- Air objective (ZEISS A-Plan 40X)

Protocol

1. This protocol is used for TPM and RNA extension experiments on AFS setup.
2. Start with a clean flow cell.
3. Bleach is flushed in for at least 10 minutes.

4. Chip is rinsed with water.
5. 250 μl of 1 mM Sodium Thiosulfate is flowed in and incubated for 10 minutes to stop bleaching reaction.
6. PBS is used to flush the Sodium Thiosulfate.
7. 30 μl of 20 $\mu\text{g}/\text{ml}$ Anti-DIG is incubated in PBS for at least 20 minutes.
8. 200 μl of PBS is flushed with 0.2% w/v BSA. This is incubated for 30 minutes.
9. 200 μl of PBS is flushed with 0.5% w/v Pluronics. This is incubated for 30 minutes.
10. PBS with 0.02% w/v casein and 0.02% w/v Pluronics is flushed. This is also the measuring buffer.
11. 30 μl of 0.05 pM DNA is flushed for good coverage.
12. PBS with 0.02% w/v casein and 0.02% w/v Pluronics is flushed.
13. 20 μl polystyrene bead (4.5 μm) is added to 1000 μL PBS with 0.02% w/v casein and 0.02% w/v Pluronics.
14. The beads are spun down for 2 minutes at 2.4 rcf.
15. Residue is removed and 1000 μL of PBS with 0.02% w/v casein and 0.02% w/v Pluronics is added again.
16. The beads are spun down for 2 minutes at 2.5 rpm.
17. Residue is removed and 20 μl of PBS with 0.02% w/v casein and 0.02% w/v Pluronics is added.
18. Beads are flushed in and the flow cell is hold upside down.
19. Beads tethering to the DNA can be observed realtime under microscope.
20. With this protocol it takes about 10 minutes for a good coverage.

21. Excess beads has to be flushed out.
22. Flushing should not be too hard since it is possible to pull of tether off or the DNA can collapse to the surface.

A.17 AFS experiment buffer preparation

These buffers are for AFS experiment. Various steps has various buffers for our experiment. The process to make all these buffers are explained one by one. 500 ml of 1 mM Sodium thiosulphate is as follows.

Materials, reagents and equipment

Reagents:

- BSA - Bovine serum albumin (EMD OmniPur, catalog numer: 2910)
- Casein (Sigma, catalog number: C6780)
- IPA - Isopropanol (EMD Millipore Corporation, Catalog number 67-63-0)
- KCL - Potassium chloride (Fisher Chemicals, catalog number: P217)
- KH_2PO_4 - Monopotassium phosphate (Fisher Chemicals, catalog number: 7778-77-0)
- Nacl - Sodium chloride (Fisher Chemical, catalog number: S271)
- Na_2HPO_4 - Disodium phosphate (Fisher Chemicals, catalog number: 7558-79-4)
- PBS - Phosphate Buffered Saline (Sigma Aldrich, product number: A9226)
- Pluronics (Sigma, catalog number: P2443)
- 1mM sodium thiosulfate (Fisher Scientific., catalog number: 10102-17-7)

Equipment:

- AFS instrument (Lumicks)
- Air objective (ZEISS A-Plan 40X)

Protocol

1. $(500 \text{ ml} * 0.001 \text{ mM} * 158.108 / 1000) \text{ gm} = 0.0790 \text{ gm} = 79 \text{ mg}$ of sodium thiosulfate in to 500 ml of water.

The process to make 10 mM PBS is as follows. Following has to be dissolved in 800 ml distilled H₂O.

1. Add 30 mg BSA in 15 ml PBS to make 0.2 gm BSA in 100 ml PBS
2. Add 0.5 gm Pluronics in 100 ml PBS to make 0.5% w/v Pluronics. So, 75 mg in 15 ml PBS.
3. Add 0.02 gm casein and pluronics in 100 ml PBS to make 0.02% w/v of casein and pluronics. So add 3 mg casein and pluronics in 15 ml PBS.
4. pH adjusted to 7.4 with HCl.
5. Sterilize by autoclaving.
6. Volume adjusted to 1L with additional distilled water.
7. 8 g of NaCl
8. 0.2 g of KCl
9. 1.44 g of Na₂HPO₄
10. 0.24 g of KH₂PO₄
11. 137 mM NaCl, 2.7 mM KCl, 10 mM Na₂HPO₄, 2 mM KH₂PO₄ in a PBS buffer.

A.18 Making AFS lookup table

Look up table are used to record the z positions of the beads. These lookup table helps us to related the position of out beads during the experiment while force is being applied. The steps used to record the look up table in an AFS setup is explained below.

Materials, reagents and equipment

Materials:

- AFS flowcell (Lumicks)

Reagents:

- Anti digoxin beads (Spherotech Inc., catalog number: TP-20-2)
- DNA (Integrated DNA technologies)

Equipment:

- Air objective (ZEISS A-Plan 40X)
- Syringe pump (New Era Pump System)

Protocol

1. After selection of all the tethered beads, Z tracking has to be done.
2. For this look up table has to be created.
3. Individual bead might look different from each other, so every bead will have its own LUT.
4. The range, amount of measuring point, delay time and amount of averages has to be chosen for the LUT.
5. The amount of measuring point in the chosen range is found to be 100 nm steps which gives the best resolution.
6. Delay time has to be set between sending a signal to the function generator and measuring the radial profile for the LUT because the stage needs some time to move to a new position. Z stage takes less than 20 ms to move 100 nm.

7. The amount of average of the radial profile has to be set because each image contains a certain amount of noise and the noise can be reduced by averaging the LUT images. The more averages taken, the longer it takes to make the LUT and the more drift we include making the LUT.
8. Perfect focus system should be turned off when making a LUT.
9. Reasonable force has to be applied on the beads. The force needed depends on the construct, but roughly 10 pN should be okay.
10. Checks can be performed before starting measurement by setting the focus in the middle of measured LUT. Also checking can be done to see if LUTs look smooth and if the beads respond when a force is applied on them.